2019

A Study on Erosion Resistance for Microbially Induced Calcite Treated Beach Sand

Abigail Chek
n01399405@unf.edu

A STUDY ON EROSION RESISTANCE FOR MICROBIALLY INDUCED CALCITE TREATED BEACH SAND

By

ABIGAIL M. CHEK

A DISSERTATION PRESENTED TO THE GRADUATE SCHOOL
OF THE UNIVERSITY OF NORTH FLORIDA IN PARTIAL FULFILLMENT
OF THE REQUIREMENTS FOR THE DEGREE OF
MASTER OF SCIENCE IN CIVIL ENGINEERING

UNIVERSITY OF NORTH FLORIDA

2019

This thesis titled “A Study on Erosion Resistance for Microbially Induced Calcite Treated Beach Sand” written by Abigail M. Chek has been approved by:

____
Raphael Crowley, PhD PE

____
Donald Resio, PhD

____
Terri Ellis, PhD

To my family

ACKNOWLEDGMENTS

I am forever grateful for the grace of God and the blessings He has bestowed upon my life. He has given me the strength, knowledge, and the ability to persevere throughout my time in graduate school, particularly during the development of this research study. Without His blessings, this achievement would not have been made possible.

Thank you to the staff at the University of North Florida, particularly the Taylor Engineering Research Institute (TERI) and the Biology Department. I would especially like to extend profound gratitude to Dr. Crowley for serving as my thesis advisor. His unwaivering support and continuous feeback throughout the development of this project made this research possible. I would also like to thank Dr. Resio and Dr. Ellis for the support they provided me as members of my thesis committee. I would like to thank Michael Durnin and Olivia Wright, students at the UNF Biology Department for their assistance during experimental testing. In addition, I would also like to thank Jon Berube and Josh Sasser, my fellow coastal engineering classmates for their assistance in the application process. Special thanks to the personnel at the UNF Environmental Center, especially Dave Lambert and James Taylor for their support of this research; this work was partially funded by a UNF Environmental Center Seed Grant.

Thank you to the U.S. Navy Ocean Facility Program and the Civil Engineer Corps for granting me the opportunity to attend graduate school at the University of North Florida. My time here has been unforgettable; I am looking forward to returning to the fleet with the knowledge gained here so that I may better serve this great country.

Finally, I would like to thank my family, friends, and mentors who believed in me throughout my time in graduate school. Without their everlasting support and continued encouragement, none of this would have been made possible—it truly does take a village.

TABLE OF CONTENTS

page

LIST OF TABLES

LIST OF FIGURES

Figure page

Abstract of thesis Presented to the Graduate School
of the University of North Florida in Partial Fulfillment of the
Requirements for the Degree of Master of Science in Civil Engineering

A STUDY ON EROSION RESISTANCE FOR MICROBIALLY INDUCED CALCITE TREATED BEACH SAND

By

Abigail M. Chek

December 2019

Chair: Raphael Crowley, PhD PE
Major: Civil Engineering

Microbially-induced calcite precipitation (MICP) was used to treat several “sandboxes” filled with naturally occurring beach sand collected from Atlantic Beach, FL. Unlike most previous MICP studies, a surface-spray technique was used to treat these sandboxes where relatively high-concentration bacteria solution and high-concentration calcium chloride/urea solutions were applied directly to the boxes’ surfaces. Several different treatment combinations were tested whereby bacterial optical density, bacteria/urea/calcium chloride volume relative to void space, and bacteria/urea/calcium chloride ratio were manipulated. Treated sandboxes were tested for erodibility using a pocket erodometer and for calcification using a wash method. In addition, sandboxes were dissected after calcification/erosion testing to examine calcification depth. Results showed that higher optical densities, higher bacteria quantities relative to void volume, and higher bacteria quantities relative to urea led to higher calcification. By maximizing these three variables, calcium carbonate precipitation of approximately 6% was achieved after one treatment. After five treatments, calcification was greater than 15%. However, even with significant calcification like this, erodibility improvements were relatively moderate. In addition, correlations were developed that appeared to show indirect relationships between erodibility and

calcite content; and direct relationships between calcification depth and calcite content. Overall, results seem to present a roadmap for upscaling microbial treatment for erosion control – generally, "more is better" and "shocking" the soil with high amounts of bacteria, urea, and calcium carbonate may produce the most erosion resistance.

CHAPTER 1
INTRODUCTION AND BACKGROUND

1.1 Beach and Dune Erodibility

The state of Florida is comprised of 825 miles of sandy beaches fronting the Atlantic Ocean, Straits of Florida, Gulf of Mexico, and the roughly 66 coastal barrier tidal inlets. According to an annual report published in June of 2019 by the Florida Department of Environmental Protection (FDEP), 419.6 miles of those 825 miles of shoreline are critically eroded beaches. These include 8.7 miles of critically eroded inlet shoreline, 90.9 miles of non-critically eroded beach and 3.2 miles of non-critically eroded inlet shoreline statewide (Green, 2019). Figure 1-1 illustrates statewide areas of critically and non-critically eroded shoreline. According to Green (2019), pursuant to rule 62B-36.002(5), Florida Administrative Code (F.A.C.), defines "critically eroded shoreline" as a segment of shoreline where natural processes or human activity have caused a level of erosion that threatens substantial development, recreation, cultural, or environmental interests (Green, 2019).

To determine if a segment of shoreline is critically eroded, the Florida Department of Environmental Protection (FDEP) coastal engineering department investigates an area and uses both qualitative assessments and quantitative data. The type of quantitative data used by the coastal engineering staff includes an analysis of beach and offshore profiles, upland topography, nearshore and offshore bathymetry, historical shoreline position changes, storm tide frequency, beach and dune erosion, recent storm damage, design capability of offshore development, and the proximity of development, infrastructure, and wildlife habitat to the effects of a 25-year frequency storm event. According to Green (2019), only beaches that are exposed to the open water of the Gulf of Mexico, Atlantic Ocean, or Straits of Florida, and are not sheltered by a coastal barrier or island shoal, are considered part of the Florida coastlines (Green, 2019).

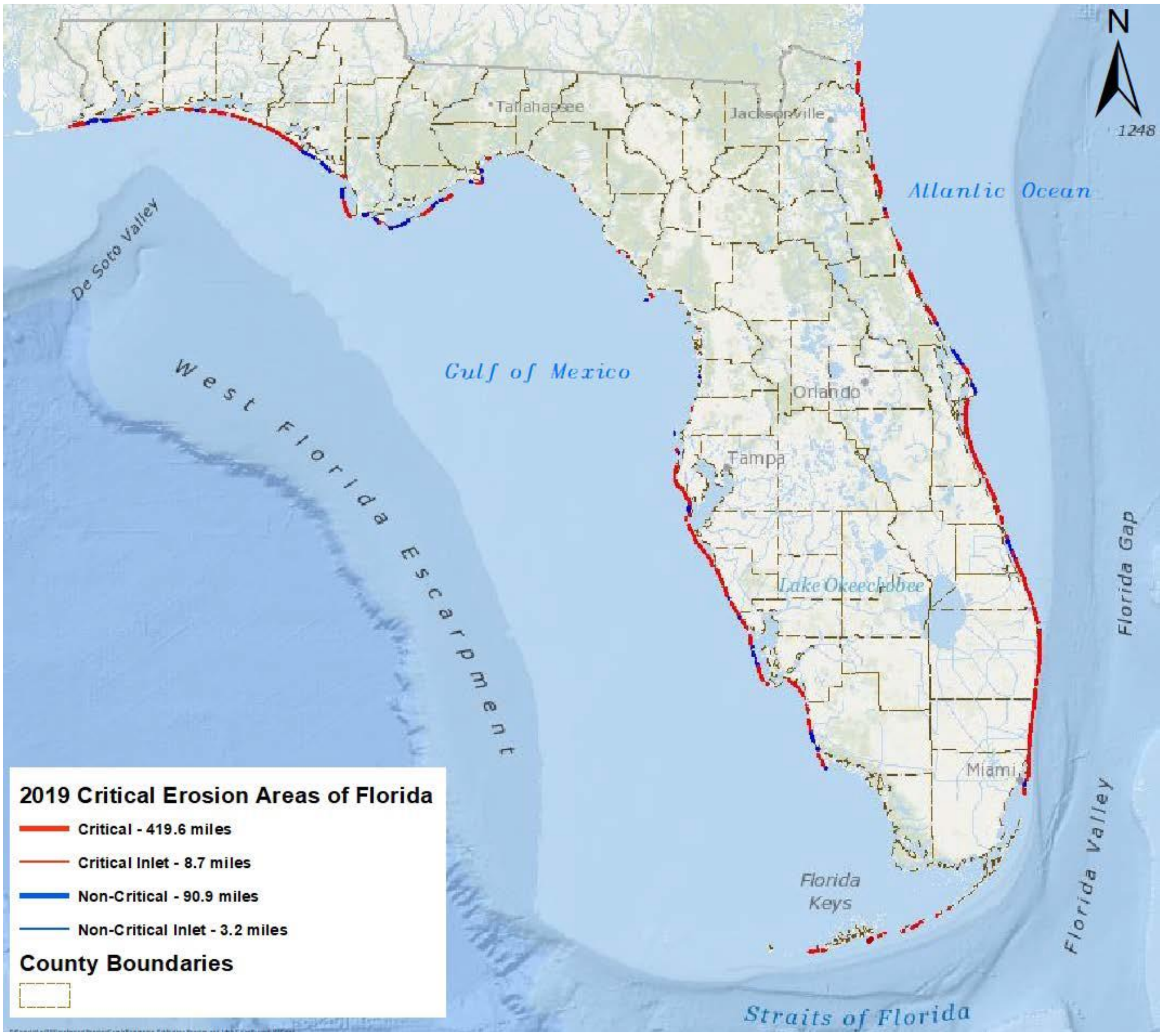

Figure 1-1. Statewide areas of critically and non-critically eroded shoreline provided by Florida Department of Environmental Protection, Division of Water Resource Management.

1.1.2 Recent Hurricane Impacts on Florida Coasts

In 2016, Hurricane Matthew and Hurricane Hermine caused significant erosion effects on Florida's coastlines, specifically the sand dunes along the Northeast Florida coastline. This catastrophe was quickly proceeded by Hurricane Irma in 2017 which continued to ravish Florida's Northeast coastline and inflict further erosion damage to the dunes. Photos from Crowley et al. (2019) are illustrated in Figure 1-2; they depict the significant coastal erosion from the effects of Hurricane Matthew and Hurricane Irma. The dune systems along the Northeast Florida coastline suffered severe erosion and, in some areas, undercutting. Sand dunes offer a surplus of environmental benefits and generally protect the coastlines from storm effects. However, due to the highly erodible nature of beach sand, they offer limited protection from erosion.

Figure 1-2. Dune damage near Flagler Beach, FL – Painters Hill (top-left and top-right); and erosion/undercutting just south of Vilano Beach, FL (bottom-left and bottom-right) (Crowley et al, 2019)

1.2 Current Hardened Structure Erosion Mitigation Methods

Over the years, several mitigation measures have been used in various attempts to mitigate or prevent coastal erosion. While some of these measures are effective, each has its own negative consequences. These traditional shoreline stabilization techniques are discussed below:

1.2.1 Seawalls, Bulkheads, and Other Wall Structures

Seawalls, bulkheads, and other wall structures are the most common type of hard stabilization structure against beach erosion within the state of Florida and are used to protect shorelines from the impacts of normal wave action. Common building materials for these structures include timber, steel, rock, concrete, or polymers. Evidence from Hurricanes Irma and Matthew appear to indicate that wall-type structures are effective in terms of beach protection (Crowley et al. 2018; Hudyma et al. 2018). However, these structures are not without their issues. First, under worst-case storm conditions, wall-type structures may overtop, which could lead to failure. After Hurricanes Irma and Matthew, the National Science Foundation (NSF) Geotechnical Extreme Events Reconnaissance (GEER) team noted that performance was significantly affected continuity in the sense that any "holes" or "gaps" in bulkheads tended to also lead to upland erosion and failure (Hudyma et al. 2018). Generally, when walls are installed, the beach on the shoreside of the structure will erode and, in some cases, shoreside beaches may be lost entirely. This may negatively affect beach-centric tourism environment or result in destruction of wildlife habitats (Bush, 2004).

1.2.2 Breakwaters

An alternative to wall-type structures are breakwaters. While their primary purpose is wave attenuation, an added benefit to breakwaters in the context of beach protection is sediment accumulation between the beachfront and the breakwater. Two specific types of breakwaters that have become increasingly popular are fixed breakwaters and submerged breakwaters. An example of a submerged breakwater is an artificial reef or a structure built on the seafloor. As more of these breakwater structures are put into place, many of their disadvantages have become apparent. Fixed breakwaters are permanent structures that require continuous maintenance which can become expensive. In addition, fixed breakwaters are typically a displeasing sight to a popular shoreline, ultimately effecting the beachfront tourism industry. Alternatively, a submerged, artificial reef placed too close to the shoreline may result in shoreline erosion (Ranasinghe, 2006). While breakwaters can be best suited to protect port and harbor entrances from added silt build up, they provide little benefit as an erosion control method to a pre-existing shoreline.

1.2.3 Groins and Jetties

In the state of Florida and along many coastlines of the United States, jetties and groins are sometimes used to prevent beach erosion. Groins are walls generally built perpendicular to the shoreline used to trap and hold sediment flowing in the long shore current. Jetties and groins are also built as T-shaped, Y-shaped, zigzag shaped, and angled from shore. They are typically placed in groin fields, which are multiple groins that extend like fingers away from shore (Anderson, 2009). Materials used to build these structures include rock, concrete, wood, steel, and fabric bags filled with sand. They are intended to combat the problem of existing sediment erosion. In the state of Florida, these structures are typically found along the east coast. Many disadvantages exist with the placement of groins or groin fields. Updrift beaches are widened by this method, while downdrift beaches become starved of sediment. In addition, the entrapment of sediment on one side of the groin intensifies erosion on the other (Bush, 2004).

1.2.4 Riprap and Shore Armoring

Riprap is another man-made shore stabilization technique used to armor a shoreline against wind and wave erosion and scour. Riprap is simply a method of layering rock across a threatened area to prevent further erosion. Typically, riprap is made of angular rock, rubble, or broken concrete slabs. Riprap can be strategically placed by hand or simply dumped in an area to form a revetment and protect from erosion and scour (Brown, 1989). Generally, riprap revetments are designed to have an appropriate slope and rock size to adequately protect an area from erosion, typical slope ratios are 1:2 (vertical to horizontal) or 1:3. Layers of smaller stone or gravel are placed under and between the larger rock to help reinforcement. Like other traditional shoreline stabilization techniques, riprap also has some negative issues. Often, riprap projects along the coast are faced with ongoing repair and maintenance that become expensive and potentially problematic. Research has shown that fewer aquatic species and vegetation live in armored revetments than in natural coastal habitats (Massey, 2017). The limited vegetation degrades the wildlife and threatens the breeding areas for aquatic species. Due to the low coefficient of friction, riprap tends to increase the wave celerity in the water which ultimately increases erosion on adjacent shorelines and scour at the toe ends of the embankment making it a counterintuitive shore stabilization method (FEMA, 2009). Lastly, riprap has similar issues to wall-type structures in the sense that riprap often may replace beaches and negatively affect beach tourism.

1.2.5 Beach Nourishment and Dune Benefits

As noted above, each method of structural beach protection has its disadvantages. In recent years, several communities have moved away from structural-type protection measures in favor of beach nourishment (Dean, 2003). This leaves sand dunes as the primary line of protection against erosion, upland flooding, and upland damage. Dunes are also excellent for the environment. In Florida in particular, sand dunes are the primary location for sea turtle nesting and the home of many other wildlife species. Additionally, dunes and ongoing beach nourishment projects positively impact beach tourism. However, dunes are highly erodible and overall are very susceptible to failure during large-scale storm events. It would be beneficial if there were a sustainable, rapidly-deployable mechanism that could be used to strengthen dunes to make them less susceptible to erosion and scour.

1.3 Microbially-Induced Calcite Precipitation Introduction

In recent years, Microbially-Induced Calcite Precipitation (MICP) has emerged as a sustainable method for strengthening clean sands. This technology began in the early 1990s; Sumner (1926) was the first to crystallize the enzyme urease from a jack bean to use as a method for increasing oil well yield. The enzyme urease is the catalyst for the MICP reaction that is most commonly used today (Mobley et al. 1995). In the early 2000s, the research group at UC Davis began looking to adapt MICP for use as a method for liquefaction control during hurricanes (DeJong et al. 2006). Since then, MICP has been used in several soil strengthening applications (Cheng et al. 2013; DeJong et al. 2010; Maleki et al. 2016; Martinez et al. 2013; Montoya et al. 2015; Mujah et al. 2017; Ng et al. 2015; Salifu et al. 2016; Sharma & Ramkrishnan 2016; Soon et al. 2013; Van Paassen et al. 2010; Whiffin et al. 2017; Zhao et al. 2014). More recently, research groups at the University of North Florida (UNF) and North Carolina State University (NC State) have begun exploring using MICP as a method of erosion control – particularly for clean, sandy beaches and dunes.

Specifics associated with MICP are discussed in detail in Chapter 2. Briefly, MICP involves either stimulating naturally-occurring geomicrobes to produce calcite or supplementing already present geomicrobes with ureolytic bacteria (usually *Sporosarcina pasteurii*) and inducing them to produce calcium carbonate. This calcite bonds soil particles together (Saniflu et al. 2016). The constituents associated with MICP are all sustainable ingredients – calcium chloride solution, urea, and naturally-occurring harmless bacteria. Mortensen et al. (2011) conducted a comprehensive study of environmental factors of MICP. Results from the study showed that the ureolytic bacteria can grow in a variety of groundwater environments including different types of freshwater and various levels of salinity and the bacteria is harmless to the surrounding environment.

1.4 MICP for Beach Stabilization

Using MICP as a method for erosion control is still relatively new. While countless researchers have shown strength improvements for MICP-treated soil, there is limited information of the known correlation between soil strength and erodibility (Mehta, 1991; Montoya et al. 2018). As such, erosion improvement must be quantified independently from strength. Shanahan et al. (2016) conducted a study using sandbox models which represented sand dunes that were treated with MICP. In Shanahan's study, the bacteria and feedstock were introduced to the surface of the sandboxes and then allowed the bacteria to permeate through the soil matrix. Once applied, the specimens were placed at specific angles to simulate sand dunes and were subjected to wave action using a wave tank. The weight of the samples was recorded both before and after they were subjected to the wave action. According to Shanahan et al. 2016, the difference in mass before and after the wave tank was the amount of erosion that acted on the sample. This study provided follow-on researchers with significant preliminary information on MICP as an erosion mitigation technique. Results showed that MICP treatment appeared to reduce erosion to some extent. However, it is unclear how these results translate to real-world conditions in the field. In particular, the wave tank tests were conducted using scaled waves on the order of four inches. Orbital velocities associated with these waves would be relatively small when compared with orbital velocities associated with prototype-scale waves. As such, bed shear stresses under prototype-conditions will be much higher than bed shear stresses observed during the small-scale wave experiments. While erosion reduction was observed during the scaled tests, it is difficult to extrapolate these results to larger scales without quantifying erosion index using a more “standard” methodology since sand grain-size cannot be scaled in a laboratory

Like Shanahan et al. (2016), Crowley et al. (2019) conducted a similar study utilizing a small-scale model of a dune treated with MICP. Using a simple spray nozzle technique, the bacteria and feedstock were applied directly to the dune surface and allowed to cure for 48 hours. Once air-cured, the treated dunes were analyzed using a sieve analysis and calcium carbonate content testing. Dissection of the treated dunes revealed significant hardening of the interior and the formation of large blocks of “cemented” material within the sand. Additionally, Crowley et al. (2019) discovered that the mean grain size diameter increased after being treated with MICP. The untreated sand had a D_{50} of 0.2 mm whereas the treated sand had a D_{50} of 0.6 mm. This increase in median grain size is slight and may indicate that MICP does not have a significant effect on erosion mitigation. But again, it is difficult to extrapolate these results without quantifying standard erosion indices.

Montoya et al. (2018) better characterized erodibility for MICP-treated specimens using jet testing similar to the testing performed by Hanson (1990), Hanson and Cook (1997), and Hanson (2001). These tests were conducted upon poorly graded beach sand which is known to be very highly erodible. Specimens were treated with urea (0.33 M), ammonium chloride (0.374 M) and relatively small amounts of calcium chloride (0.05 M). Initial bacterial optical density (OD) ranged between 1.0 and 1.2. All treatments were conducted by completely filling the soils’ void volumes. Results showed that MICP treatment could reduce erodibility, but to decrease erodibility significantly, multiple treatments were needed.

Most recently, Ghasemi et al. (2019) conducted a study to quantify erodibility as a function of relative concentrations of urea and calcium chloride. Slightly stronger solutions were used when compared to the Montoya et al. (2018) study; $CaCl_2$ was fixed at 1 M while urea was varied between 2 and 3 M. Similar to the Montoya et al. (2018) study, void volumes were 100% saturated throughout testing. Results showed that greater erodibility improvements were achieved for higher relative urea concentrations. Overall, these most-recent studies show that it should be possible to optimize erosion improvement by manipulating factors associated with MICP treatment.

1.5 Standard Erosion Rate Testing Techniques

To better quantify potential erosion improvement for MICP-treated dunes, more testing was required. Erosion testing is a well-established field which gained momentum in response to the scour problem in the 1990s. Eventually, several established erosion tests were developed that allowed engineers to relate flow rates in the field to erosion. The crux of this method hinges upon the following relationship first proposed by Einstein and Krone (1951):

$$E = M(\tau - \tau_c) \tag{1-1}$$

where E is erosion rate; τ is the bed shear stress; τ_c is the critical shear stress; and M is a material-specific erosion constant. Relationships similar to Eq. 1-1 may be developed for any bed material; these relationships are known as "erosion functions." Then, stresses in the field are estimated using various techniques – often by coupling results from computational fluid dynamics with conservative hydrographs. Each field stress condition is converted to an erosion condition based upon the bed material's erosion function. Total erosion is found by summing all erosion events over the lifetime of an analysis. Tests associated with erosion function development are discussed in detail in Hydraulic Engineering Circular No. 18 (HEC-18; Arneson et al. 2012) and summarized below:

1.5.1 Piston-Style Erosion Rate Testing Devices

Piston-style erosion rate testing devices involve inserting a sediment specimen, often a Shelby tube, into a duct with a false bottom, and running water over the exposed specimen's surface (see Figure 1-3 below). As the specimen erodes, it is advanced using a piston so that its top-surface remains level with the duct bottom. Erosion rate is simply the rate of piston advancement. Shear stress is estimated using boundary-layer theory. Several piston-style instruments have been developed over the years including the SedFlume (McNeil et al. 1996); the ASSET (Roberts et al. 1998); the EFA (Briaud et al. 2001); and the SERF (Crowley et al. 2012).

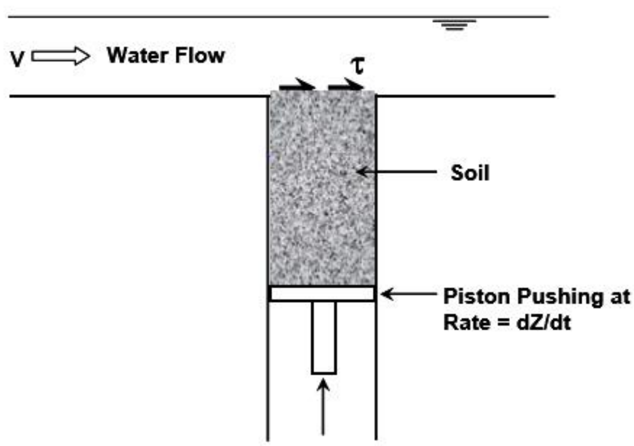

Figure 1-3. Schematic diagram of piston-type erosion rate device (Arneson et al. 2012)

1.5.2 The Rotating Erosion Testing Apparatus (RETA)

Rotational-style tests are another erosion function measurement apparatus that are more-suitable for stiffer sediments and rock cores. In these instruments, a specimen is obtained and inserted into a cylindrical cup. The cup's annulus is filled with water and the cup is spun around the specimen – thereby imparting a stress along the specimen's side walls (see Figure 1-4 below). Erosion rate is simply the mass of the specimen before and after the test divided by time.

Stress is usually measured with a torque cell that is attached to the specimen. Examples of rotational-style instruments are discussed by Alizadeh (1974), Bloomquist et al. (2012), Chapius and Gatien (1986), Henderson (1999), Kerr (2001), Moore and Masche (1962), Rektorik and Smerdon (1964), and Sargunam et al. (1973).

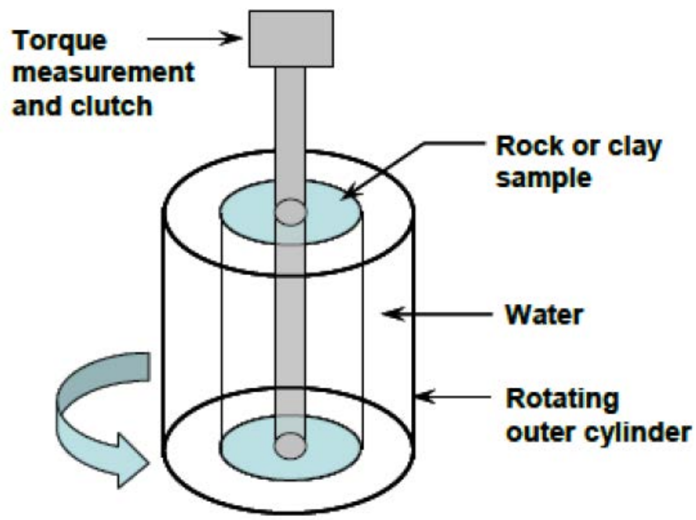

Figure 1-4. Schematic of rotational-style device (Arneson et al. 2012)

1.5.3 The Jet Erosion Test (JET)

The Jet Erosion Test (JET) is the third "standard" method used to determine erosion functions. A JET can be conducted with a remolded sample in a laboratory or in situ soil conditions with a slope less than 26 degrees. The JET apparatus consists of the following parts: jet tube, adjustable head tank, point gauge, nozzle, pump, jet submergence tank, lid, and hoses, as shown in Figure 1-5 (Hanson, 1990). A large water source must be present to conduct in situ testing. A metal cylinder is driven into the surface layer of the soil to provide a seal for the jetting tank which is filled with nearby water. Water is pumped into the head tank until the elevation is constant. Then, a nozzle is aimed at the surface of the soil. The depth of the eroded hole is measured and plotted as a function of time (Briaud et al. 2011). The equilibrium depth of the hole made by the jet in the soil is the depth which the critical shear stress is reached, and erosion stops (Hanson and Cook, 2004). The JET examines the soil in terms of the critical shear stress and erosion function for the soil. A detailed description of the JET and the testing methodology has been presented in numerous studies (Hanson and Cook, 1997; Al-Madhhachi et al., 2013).

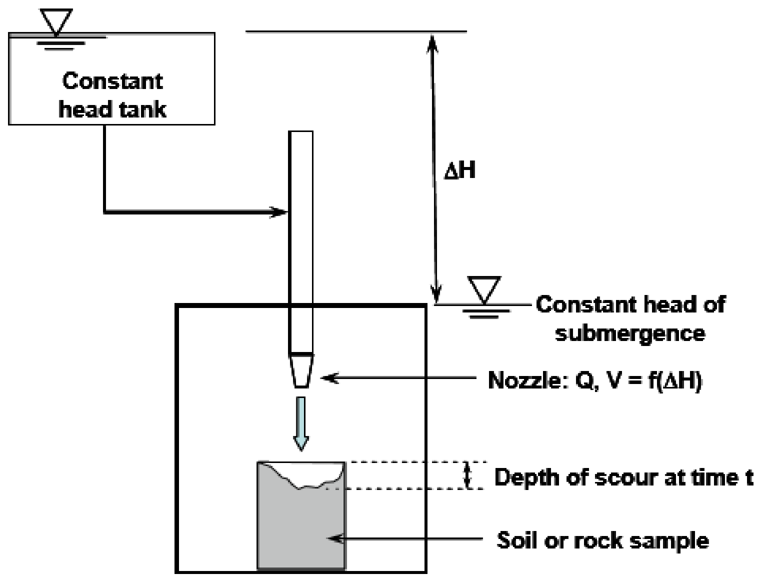

Figure 1-5. Schematic diagram of jet-type erosion rate device (Arneson et al. 2012)

1.6 Development of Erosion Indices

In 2008, the Erosion Function Apparatus (EFA) was used to classify sediment erodibility in terms of indices (Briaud, 2008). In other words, erosion rate was plotted as a function of free-stream velocity in the EFA. Several erosion categories were defined as shown below in Figure 1-6:

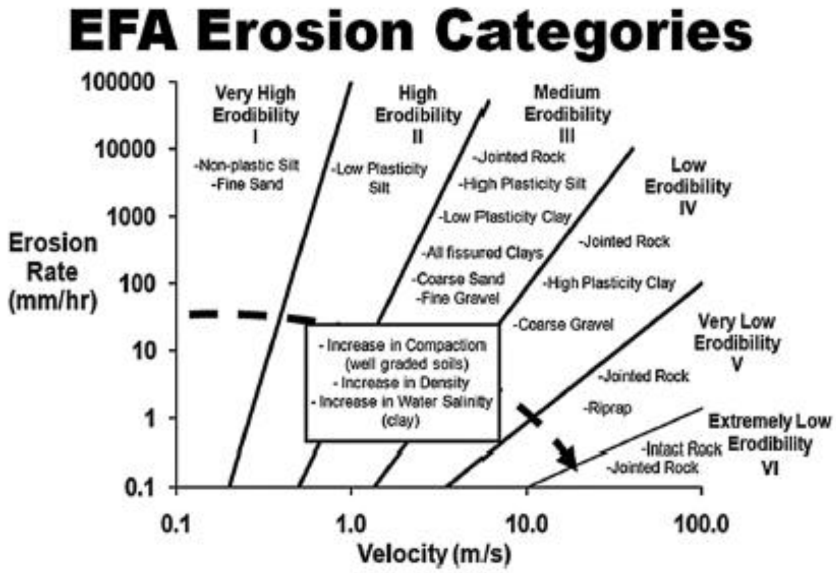

Figure 1-6. Erosion category chart (Briaud, 2008)

While not as quantitative as explicit erosion functions, the erosion index chart shown in Figure 1-6 gives a general sense of erodibility or conversely, erosion resistance. In other words, a material that is Category II, Highly Erodible, will probably erode significantly during prototype-scale waves associated with a hurricane or nor'easter. In the absence of an explicit erosion test, which requires specific equipment and may be time-consuming, understanding erosion index gives some sort of "standard' methodology that allows one to categorize erosion.

1.7 The Pocket Erodometer Test (PET)

In recent years Briaud et al. (2011) developed a simple, "real time" field test that quantifies erosion index – the Pocket Erosion Test (PET; Briaud et al. 2011). The PET is a device which generates mini jet impulses of water at a constant velocity. These impulses are aimed at the soil and an erosion hole is formed where the soil had been impacted. Briaud et al. (2011) used the EFA and PET to relate PET penetration depth directly to erosion indices associated with Figure 1-6. Thus, erodibility could be estimated qualitatively, directly, relatively quickly and related to stresses associated with field conditions.

1.8 Goals and Objectives

The overall goal of this research was to quantify erodibility for MICP-treated specimens in terms of erosion indices. Specimens were treated using a surface-spray technique because under field conditions, such a technique would appear to be the most realistic way to spread MICP solutions onto dunes. Optimization testing was conducted both in terms of initial bacterial optical density and solution volume as a function of pore space. Results, which will be presented in detail in Chapter 3, showed that erodibility was lowest when specimens were fully saturated with MICP ingredients, but even under these conditions, erodibility only moved from Category I, Very High Erodibility to Category II, High Erodibility. As such, under field-conditions, it is unlikely that a one-time MICP treatment of a dune system will significantly reduce erosion. In an effort to determine what it would take for MICP to "move the needle further" (i.e., move erodibility below Category II), several sandboxes were treated multiple times.

1.9 Thesis Organization

This thesis is organized into five parts:

- Chapter 1 presents the introduction, background information and the motivation for research.
- Chapter 2 presents the methodology, the materials and methods used throughout this research including treatment techniques and erodibility categories.
- Chapter 3 of this thesis presents the results from the various studies and the outcomes that were further explored for a more thorough analysis.

- Chapter 4 presents analysis of the results shown in Chapter 3.
- Chapter 5 presents a summary and conclusions from this study and provides recommendations for future work.

CHAPTER 2
METHODOLOGY

2.1 Background

As discussed in Chapter 1, the goal of this study was to quantify erosion improvement for MICP-treated beach sand. More specifically, the goal was to quantify differences associated with various treatment variables/techniques. As such, four test series were conducted during this study: (1) Optical Density (O.D) testing, (2) soil saturation testing, (3) bacteria to feed stock ratio testing and, (4) multiple treatment testing. After each round of tests, effectiveness was quantified using pocket erosion testing (PET) and calcification testing (ASTM D4373-14).

2.1.1 Sediment Characteristics

The sediment used for the research was beach sand collected from Atlantic Beach, FL. The sand was oven dried for seven days, cooled, and a soil analysis test was conducted using ASTM C136/C136M-14 standard (ASTM 2014). This particle size distribution is shown in Figure 2-1. The average particle diameter of the sand (D50) was 0.187 mm while the D_{10}, D_{30}, and D_{60} were 0.095, 0.14, and 0.2 mm, respectively.

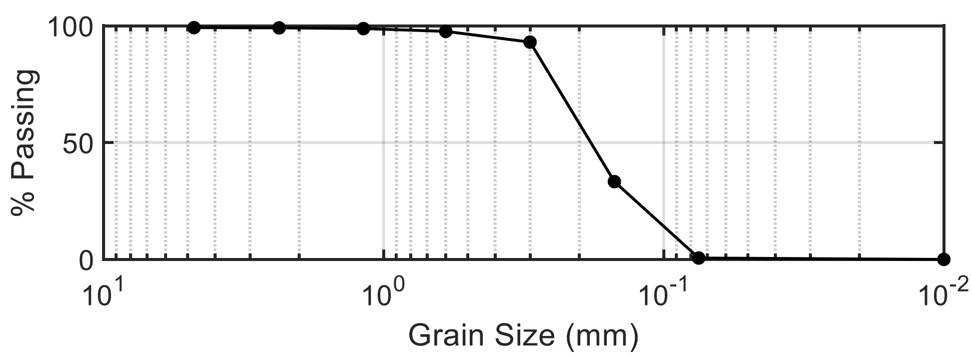

Figure 2-1. Grain-Size Distribution

Using Equation 2-1, the coefficient of uniformity (Cu) was 2.105 and using Equation 2-2 the coefficient of gradation (C_c) was 1.031.

$$Cu = \frac{D_{60}}{D_{10}} \tag{2-1}$$

$$Cc = \frac{{D_{30}}^2}{D_{60} \times D_{10}} \tag{2-2}$$

This sand was classified as poorly graded and corresponded to Unified Soil Classification System (USCS) category SP. Using ASTM D854 (2014), a standard test method for specific gravity of soils was conducted on the sand sample. Equation 2-3 and Table 2-1 outline the test below:

$$G_s = \frac{M_s G_w}{M_{fw} + M_s - M_{fws}} \tag{2-3}$$

Table 2-1. Specific Gravity Test

Specific Gravity Test	
mass of dry soil, M_s:	150 g
mass of flask + water + soil, M_{fws}:	783.5 g
Temperature:	72 °F
Specific Gravity of water @ T degrees C, G_w:	0.997754
Mass flask + Water, M_{fw} from calibration curve:	689.2 g
Specific Gravity, G_s:	2.686949731

The specific gravity on the sand sample was 2.68.

The void ratio, e, of the sand sample was laboratory calculated by utilizing a simple phase diagram shown in Figure 2-2 and Equation 2-4.

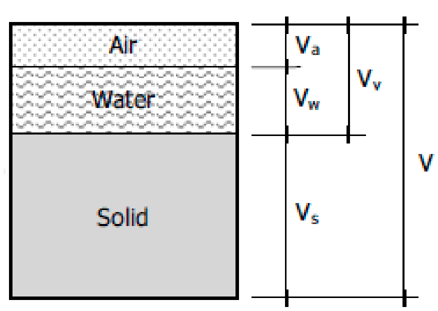

Figure 2-2: Phase Diagram

in this diagram, V_v representes the volume of voids; V_w the volume of water; V_a the volume of air; V_s the volume of solids; and V the total volume.

$$e = \frac{V_v}{V_s} \tag{2-4}$$

The soil sample was fully saturated, therefore in the phase diagram above the volume of air was zero and the void ratio was calculated using Table 2-2 and Equation 2-5.

Table 2-2. Void Ratio Calculation

Void Ratio	
V_w:	10.3 ml
V_s:	28.5 ml

$$e = \frac{V_w}{V_s} \tag{2-5}$$

The void ratio test determined that this sand had a void ratio of 0.36.

The sand was uniformly distributed into thirty 6"x 6" x 5.5" wooden boxes using an air pluviation method to produce similar relative densities (see Fig. 2-3). The V_v of the sand in the boxes was 0.1145 ft^3. Premium landscape fabric was secured to the bottom of each sand sample box to allow fluid to drain through the sandbox specimens during treatment.


Figure 2-3. Air pluviating the sand for MICP treatment

2.1.2 Microbial Induced Calcite Precipitation Governing Reactions

Governing reactions associated with MICP treatment have been detailed by several researchers. As summarized by DeJong et al. (2006), the reactions are initiated when ureolytic bacteria, usually *Sporosarcina pasteurii,* lyse urea:

$$CO(NH_2)_2 + 2H_2O \rightarrow 2NH_3 + H_2CO_3 \tag{2-6}$$

From the above reaction, the ammonia reacts with water to form ammonium ions and hydroxide ions outlined in Equation 2-7:

$$NH_3 + H_2O \leftrightarrow NH_4^+ + OH^- \tag{2-7}$$

Once Reaction 2-7 occurs, the hydroxide ions react with the carbonic acid which is formed as a result of the urea breakdown. When the hydroxide ions react with the carbonic acid, they begin to form a carbonate ion which is outlined in Equation 2-8 and Equation 2-9, respectively. The carbonate ion combines with the dissolved calcium to form calcium carbonate illustrated in

Equation 2-10. In addition, a secondary reaction occurs whereby, the calcium ions combine with the bicarbonate ion and produces calcium carbonate, carbon dioxide, and water (Equation 2-11).

$$H_2CO_3 + OH^- \leftrightarrow HCO_3^- + H_2O \quad (2\text{-}8)$$

$$HCO_3^- + OH^- \leftrightarrow CO_3^{2-} + H_2O \quad (2\text{-}9)$$

$$Ca^{2+} + CO_3^{2-} \leftrightarrow CaCO_3(s) \quad (2\text{-}10)$$

$$Ca^{2+} + 2HCO_3^- \leftrightarrow CaCO_3(s) + CO_2(g) + H_2O \quad (2\text{-}11)$$

2.1.3 MICP Constituent Preparation

Sporosarcina pasteurii NRS929 (USDA) were grown overnight from 1 ml frozen glycerol stocks on Brain Heart Infusion (BHI) agar plates and 2% urea at 30◦C. Cells were scraped from the plates to inoculate liquid cultures of Brain Heart Infusion (BHI) broth and 2% urea. Liquid cultures (1.5 liters) were grown overnight in Fernbach flasks at 30◦C and 200 rpm for continuous aeration using a shaker incubator. Liquid *Sporosarcina pasteurii* cultures were grown to an optical density (OD) of at least 2.0 for all experiments. An Eppendorf BioPhotometer plus Model 6132 spectrometer was used to measure the OD at a wavelength of 600 nm prior to each application. In an effort to provide sufficient food for the bacteria, a relatively high-molarity solution of urea and calcium chloride (2.5-M/2.5-M) was also prepared.

2.2 Application Method

Most MICP treatments have been small-scale and have primarily focused on using an injection technique in which bacteria and feed stock are fed through the soil column using a pump (DeJong et al. 2006; DeJong et al. 2010; DeJong et al. 2013; Martinez and DeJong 2013; Mortensen et al. 2011; Weil et al. 2012). However, for this study, investigators wanted to mimic treatment techniques that could be used in the field as closely as possible. Crowley et al. (2019) showed that applying MICP-bacteria and urea/calcium chloride solution via a surface spray technique produced significant calcium carbonate. As such, a surface spray technique was used throughout this study. The bacterial culture was applied to the dry sand sample boxes using a uniform velocity spray nozzle secured to a hardened structure 100 mm from the center of the sand box. Once the bacteria were applied, the urea/calcium chloride was then applied to each sandbox using the same uniform velocity spray nozzle at the same distance of 100 mm. The sample boxes were then suspended to allow filtration through the landscape fabric and air cured in a well-ventilated area for a minimum of 48 hours. After air curing at a room temperature of approximately 72˚F, the specimens were dried at 100˚C for 48 hours and cooled prior to being tested. Figure 2-4 illustrates the application process and how the bacterial culture and feedstock were measured (Fig. 2-4a); applied to the sandboxes (Fig. 2-4b and Fig. 2-4c) and how the treated sandboxes were suspended for 48 hours to allow filtration (Fig. 2-4d).

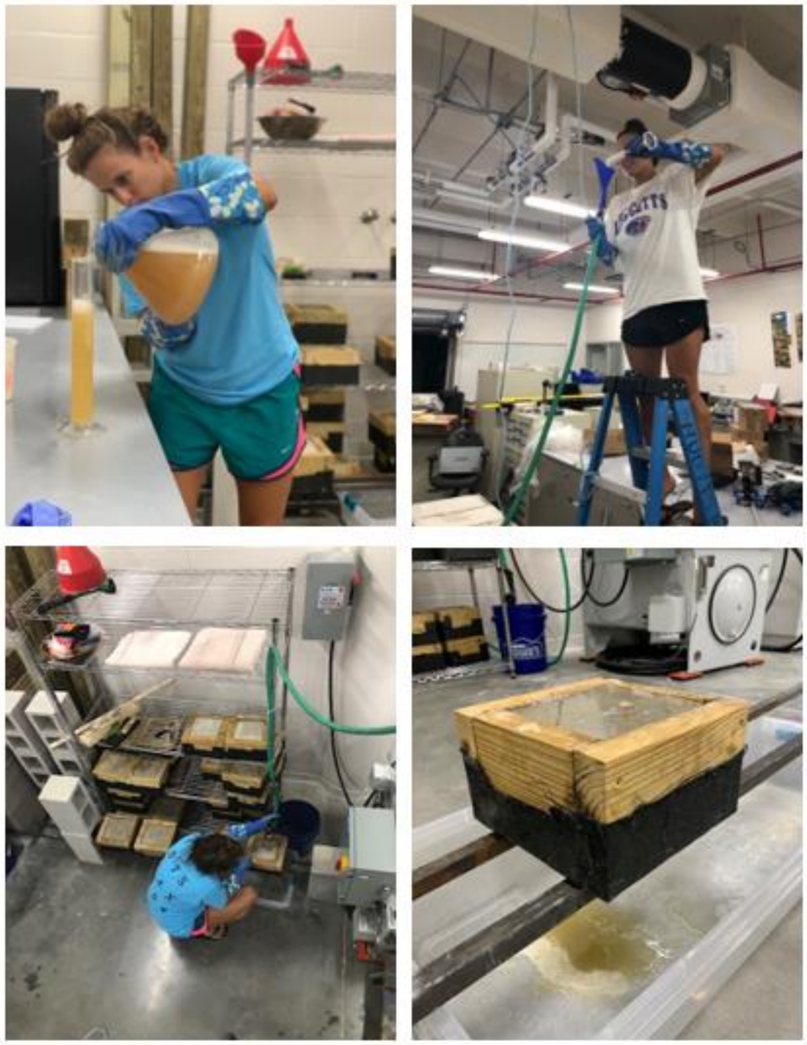

Figure. 2-4. Compilation of the testing procedure conducted. Fig. 2-4a top left, Fig. 2-4b top right, Fig. 2-4c bottom left, Fig. 2-4d bottom right.

2.3 Optimization Studies

2.3.1 Saturation Study

The erosion tests conducted within the Montoya group (Ghasemi et al. 2019; Montoya et al. 2018; Shanahan and Montoya 2016) were usually saturated. However, for this study investigators envisioned MICP as a possible treatment method for dunes upland from the waterline, and these dunes are often relatively dry. As such, this study focused on adding fluid to dry sand. It was hypothesized that there may be some optimum saturation point where either erodibility could be minimized or CCC could be maximized. The saturation optimization study was designed to test for the possible optimal point. As previously discussed, the soil analysis test determined that the sand had a void ratio of 0.36. This value was used with Eq. 2-12 to compute the volume of voids, V_v:

$$V_{voids} = \frac{V_{total} * e}{1+e} \tag{2-12}$$

Where $V_v = 0.0303$ ft^3 or 858 ml per box. Using a 1:1 ratio between urea/calcium chloride and bacteria, V_v was filled in varying increments starting at 25% saturation as shown in Table 2-2. Three ODs were examined during this portion of this study – OD = 2.01; OD = 3.01; and OD = 5.04.

Table 2-3. Saturation Study Testing Matrix

Saturation (%)	Bacteria Solution Qty. (ml)	Urea/Calcium Chloride Qty. (ml)	Total Fluid in Sample (ml)
100	429	429	858
90	386	386	772
86	369	369	738
75	329	329	657
63	268	268	536
60	257	257	515
50	291	291	582
40	172	172	343
38	163	163	326
25	146	146	292

2.3.2 OD Study

The first parameter that was conducted using the MICP treated sandboxes was an Optical Density (OD) study. Prior to each application, the bacteria cultures were tested using a calibrated spectrometer. The ODs used for this study were: 2.01, 3.01, 3.48, 5.04, and 6.79. Each optical density test was conducted on fully-saturated 1:1 specimen, meaning the ratio between bacteria and feed stock was stoichometrically balanced and the bacterial, urea, $CaCl_2$ fluid filled 100% of the pore volume.

2.3.3 Food Ratio Study

Most studies using MICP involve feeding bacteria every several hours by injecting more urea into the soil. With a surface-spray technique like the one used during this study, the bacteria are being fed only once and consume urea until they either run out or die. Investigators hypothesized that it may be possible to use fewer bacteria than the 1:1 ratio. Presumably, under these conditions, there should be less competition for food, or more food per bacteria. As such, maybe with more food, each bacteria cell could live longer and produce more calcite over time. Perhaps this increase in calcite over time could result in comparable erosion reduction when compared with erosion reduction associated with a 1:1 balance between bacteria and urea solutions. This test-series/analysis was conducted using 100% saturation and decreasing the number of bacteria relative to urea/calcium chloride as shown below in Table 2-3:

Table 2-4. Food Ratio Study Testing Matrix (V_v = Volume of Voids)

% V_v Bacteria	Bacteria Solution Qty. (ml)	% V_v $CaCl_2$/Urea	Urea/Calcium Chloride Qty. (ml)	Total Fluid in Sample (ml)
50	429	50	429	858
37.5	322	62.5	536	858
25	215	75	644	858
12.5	107	87.5	751	858

2.3.4 Multiple Treatment Study

The multiple treatment study was conducted over a span of 7 weeks. Five sandboxes were treated with bacteria and urea/calcium chloride using a 1:1 ratio and 100% saturation (i.e., 50% of the void volume occupied by bacterial solution; 50% of the void volume occupied by urea/calcium chloride). After the sand was treated, it was then air-cured for 48hrs followed by 48 hrs in an oven at a temperature of 100°C. Four of those treated sandboxes were treated again with bacteria and feed stock at a 1:1 ratio and a 100% saturation level. This treatment sequence was repeated three more times for a total of five treatments on one sample box. ODs associated with these tests varied between 3.8 and 6.9 for each of the five treatments.

2.4 Testing Methods

2.4.1 Pocket Erodometer Test (PET)

As discussed in Chapter 1, the pocket erodometer test (PET; Briaud et al. 2011) was developed to provide a quick field estimate of soil erodibility. Results from the test allow one to classify a material into 5 categories: Very High Erodibility, High Erodibility, Medium Erodibility, Low Erodibility, and Very Low Erodibility. The PET Erosion Categories are outlined in Table 2-5:

Table 2-5. PET Erosion Categories (Briaud et al. 2011)

Category Number	Category Name	PET Depth Range
I	Very High Erodibility	> 75 mm
II	High Erodibility	15 mm – 75 mm
III	Medium Erodibility	1 mm – 15 mm
IV	Low Erodibility	< 1 mm
V	Very Low Erodibility	No noticeable erosion

This test has its limitations when compared with more-quantitative erosion tests as previously discussed in Chapter 1. However, the goal of this study was to determine if MICP testing could "move the needle" for beach sand, which is known to be Category I: Very High Erodibility to another, lower erosion category where some significant erosion existence could be observed. As such, the PET is an appropriate test for this sort of analysis.

The PET is a regulated jet impulse device that is aimed horizontally at the vertical face of the sample at a specific distance for a set number of impulses (Briaud et al. 2011). The hole produced by 20 impulses of the jet stream shot from 50 mm away from the soil sample is then measured, recorded, and compared to Table 2-4 to quickly determine the erodibility category of the soil (Briaud et al. 2011). The pocket erodometer must have a specified exit velocity to ensure repeatability among each test. As determined by Briaud et al. (2011) any device that produces a velocity jet of 8 m/s, plus or minus 0.5 m/s, may be used as a pocket erodometer for testing. Briaud et al. (2011) provides guidelines for testing whether a certain water pistol is a good candidate for the PET. Calibration testing consists of pulling the water pistol's trigger 20 times at a rate of 1 squeeze per second. Then, the extents of the resultant puddle are to be measured and averaged as shown below in Figure 2-5:

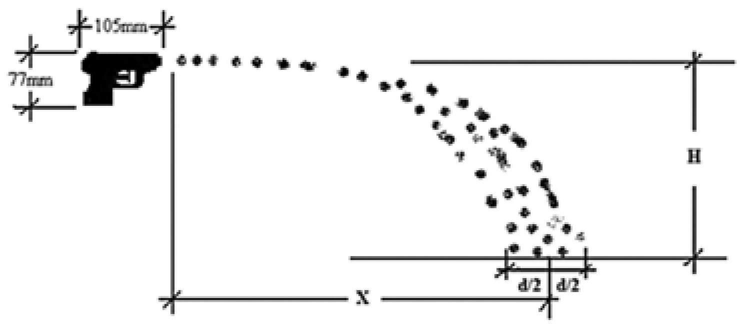

Figure 2-5. Schematic of calibration dimensions (adapted from Briaud et al. 2011)

Jet velocity is:

$$v_{0x} = \frac{x}{\sqrt{\frac{2H}{g}}} \tag{2-13}$$

where x is the average horizontal nozzle velocity, H is the fixed one-meter height, and g is the acceleration due to gravity. After testing, one water pistol appeared to consistently perform the best and is shown below in Figure 2-6.


Figure 2-6. Water pistol used for PET

Once the pocket erodometer was calibrated and verified, the sand boxes and the pocket erodometer were set up on a level surface and placed 50 mm away from one another. The pocket erodometer was used to initiate 20 jet impulses at a rate of 1 squeeze per second on each box surface, and the results were measured using a caliper. This process was repeated five times per MICP treated sand box sample to ensure repeatability. The average, standard deviation, and coefficient of variation were found from the results. A photograph of a PET being conducted during this study illustrated below in Figure 2-7.

Figure 2-7. Pocket Erodometer Test being conducted on MICP treated sandboxes

2.4.2 Calcium Carbonate Content (CCC) Test

As discussed in Choi et al. (2017), several methods may be used to determine calcium carbonate content associated with MICP-treated specimens. During this study, attempts were made to employ the calcimeter method, but results from these tests appeared to show that very little calcite was produced because the dial on the calcimeter did not deflect sufficiently to yield accurate readings. As such, the wash method was used for the remainder of the study.

The wash method procedure consisted of mixing 5 g samples with 20 mL of 1-M HCl to desolve the calcium carbonate. Then all the solution and insoluble solid were washed by distilled water on filter paper for 10 minutes each. After washing, the specimen was oven dried and its mass was measured. The difference in weight between the original sand sample (A) and the post washing sample (B) was the mass of the calcium carbonate. The calcium carbonate concentration (CCC) was calculated as illustrated in Equation 2-14:

$$CCC(\%) = 100 - \left(\frac{B}{A}\right) \times 100 \qquad (2\text{-}14)$$

This process was repeated five times per sandbox sample to ensure repeatability. The average, standard deviation, and coefficient of variation were found from the results. Figure 2-8 is a photograph of a CCC test that was conducted for this research, the MICP treated soil is mixed with the HCl prior to being washed and oven dried.

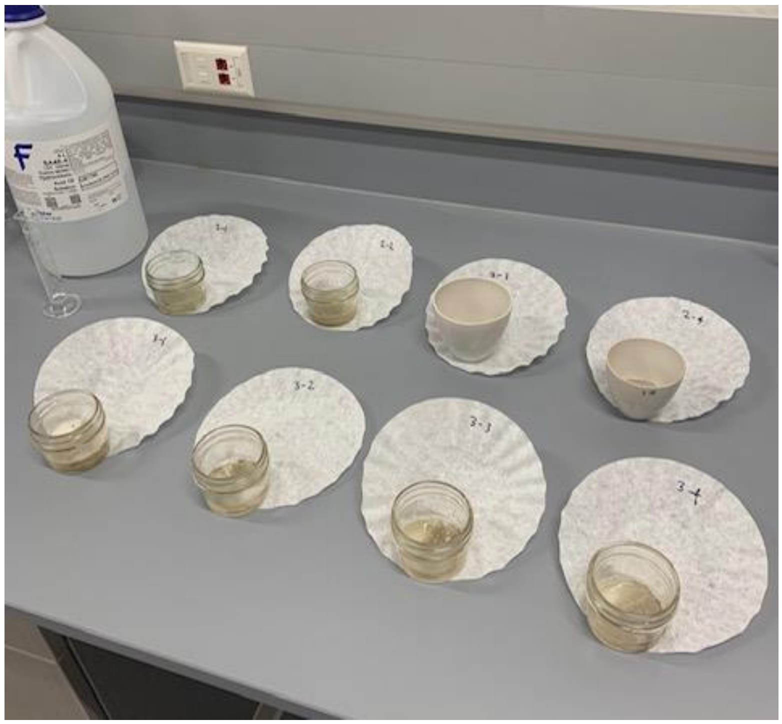

Figure 2-8. MICP treated soil mixing with HCl for a CCC test.

Beach sand from Atlantic Beach is known to have significant shell content, and shells are made from calcium carbonate. Investigators realized that the acid wash test was also dissolving calcium carbonate associated with these shells. Therefore, several control tests were also conduced on untreated sand. Results from these control tests showed that CCC for untreated sand was 5.11%. This 5.11% was deducted from acid wash CCC results so that only MICP-induced calcium carbonate was reported in the data.

According to Choi et al. (2017), CCC results produced by the washing method are 25.2% higher than the average values using one of the other five methods. However, for a study in which only qualitative comparison is required such as this one, it does not make a difference which method is used if it is used consistently (Choi et al. 2017).

2.4.3 MICP Treatment Depth Test

After the PET and CCC tests were complete, the sandbox samples were disassembled to observe and measure the depth of MICP application inside the sandbox. Using a caliper, three depth measurements per sandbox were recorded, and averaged to ensure repeatability. The standard deviation, and coefficient of variation were found from the results. Figure 2-9 is a photograph of a treatment depth test being conducted.

Figure 2-9. Depth test being conducted on sandbox sample.

CHAPTER 3
RESULTS

This chapter presents the results from the four-test series that were conducted during this research. The first section presents the results from the Optical Density (OD) testing; section two presents the soil saturation testing; section three presents the bacteria to feed stock ratio testing and section four presents the results from the multiple treatment testing. In all cases, PET depth, CCC, and strong calcification depth were plotted as a function of each optimization quantity and best-fit regression lines were fit to the data. In addition, PET depth was plotted as a function of CCC and best-fit regression lines were fit to these data as well.

3.1 Optical Density (OD) Test Results

3.1.1 OD Characteristics

The *Sporosarcina pasteurii* cultures took approximately four days to fully grow. The bacteria were grown at 30˚C with continuous aeration using a shaker incubator. Once the cultures were grown and the OD was tested and confirmed, the application process began. Qualitatively, the *Sporosarcina pasteurii* cultures with the higher OD were more potent, meaning they had a noticeably stronger ammonium scent than those with a lower OD. Additionally, the broth coloring appeared to darken as OD increased. Treatment procedures described in Chapter 2 were repeated for each sandbox/OD. After treatment, each sample visually appeared to be almost identical.

3.1.2 OD PET Depth Results

The five sandboxes treated at various ODs were subjected to several PETs. Prior to testing, the pocket erodomoeter's jet velocity was verified. Jet velocity was approximately 8.02 $\frac{m}{s}$ which is within the appropriate jet range described by Briaud et al. (2011). Five PET erosion tests were conducted on each of the sandboxes to ensure repeatability. The PET depth, average, standard deviation (σ), and coefficient of variation (COV) are illustrated below in Table 3-1 while a chart showing the PET depth as a function of initial OD is shown below in Figure 3-1.

Table 3-1. Various OD PET Results

OD:	**2.01**	**3.01**	**4.68**	**5.04**	**6.79**
Test #	PET DEPTH (mm)	PET DEPTH (mm)	PET DEPTH (mm)	PET DEPTH (mm)	PET DEPTH (mm)
1	25.01	25.01	26.38	23.01	21.46
2	27.84	27.84	25.46	23.4	21.09
3	29.31	29.31	26.1	24.5	20.91
4	28.41	28.41	27.85	23.06	21.11
5	28.82	28.82	28.12	23.1	22.46
AVG	27.878	27.878	26.782	23.414	21.406
σ	1.6917	1.6917	1.1517	0.6258	0.622
COV	6.0684	6.0684	4.3001	2.6729	2.9055

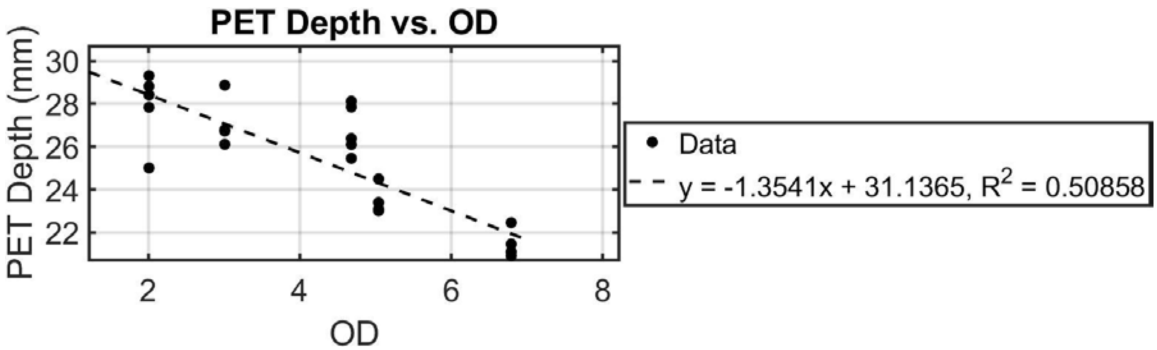

Figure 3-1. PET Depth vs. OD

3.1.3 OD Calcification Results

Following the PET, the Calcium Carbonate Content (CCC) test was conducted as outlined in Chapter 2. Four CCC tests were conducted on the top surface of each of the 100% saturated sandboxes. The CCC results from each sandbox, the average, σ, and COV were recorded and 5.11% was deducted from the results so that only MICP-induced calcium carbonate was reported in the data, results are below in Table 3-2. A chart showing the CCC as a function of initial OD is shown below in Figure 3-2.

Table 3-2. Calcium Carbonate Content test results for each OD sandbox at 100% Saturation.

OD:	2.01			3.01			4.68			5.04			6.79		
TEST #	sand sample (g)	post treated sand (g)	CCC (%)	sand sample (g)	post treated sand (g)	CCC (%)	sand sample (g)	post treated sand (g)	CCC (%)	sand sample (g)	post treated sand (g)	CCC (%)	sand sample (g)	post treated sand (g)	CCC (%)
1	5.00	4.23	10.29	5.01	4.22	10.66	4.98	3.98	14.97	5.06	4.08	14.26	5.01	3.95	16.05
2	5.02	4.24	10.43	5.02	4.23	10.63	5.01	4.29	9.26	4.99	4.00	14.73	5.01	4.03	14.45
3	5.01	4.29	9.26	5.00	4.24	10.09	5.00	4.24	10.09	5.01	4.07	13.65	5.03	4.00	15.37
4	4.99	4.27	9.32	5.01	4.26	9.86	5.03	4.29	9.60	4.99	3.99	14.93	5.01	4.04	14.25
AVG	5.01	4.26	9.82	5.01	4.24	10.31	5.01	4.20	10.98	5.01	4.04	14.39	5.02	4.01	15.03
σ	0.01	0.03	0.62	0.01	0.02	0.40	0.02	0.15	2.68	0.03	0.05	0.57	0.01	0.04	0.83
COV	0.00	0.01	0.06	0.00	0.00	0.04	0.00	0.04	0.24	0.01	0.01	0.04	0.00	0.01	0.06

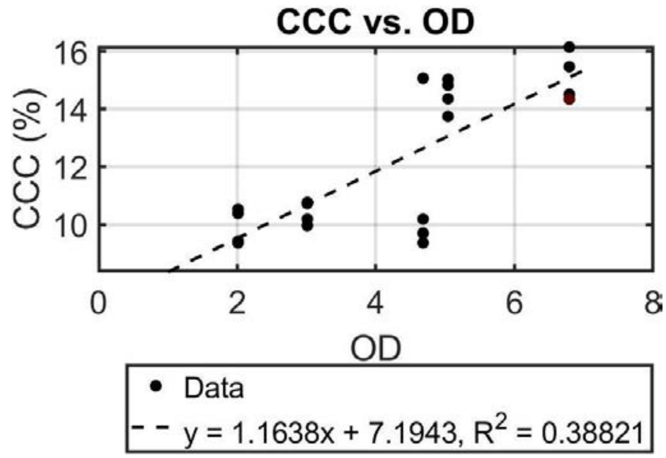

Figure 3-2. CCC (%) vs. OD

3.1.4 OD Treatment Depth Test

Once the PET and CCC tests were complete, the sandboxes were disassembled to observe and measure the depth of strong calcification inside the sandbox. The five sandboxes were disassembled, and the treatment layer was measured with a caliper. The results are outlined in Table 3-3 below and a plot showing the average depth as a function of initial OD with a best-fit regression line is illustrated in Figure 3-3.

Table 3-3. MICP application depths for varying ODs

100% SATURATED SANDBOXES					
OD:	2.01	3.01	4.68	5.04	6.79
TEST #	MICP APPLICATION DEPTH (mm)	MICP APPLICATION DEPTH (mm)	MICP APPLICATION DEPTH (mm)	MICP APPLICATION DEPTH (mm)	MICP APPLICATION DEPTH (mm)
1	101.33	108.09	121.81	111.72	121.81
2	105.94	101.92	111.53	115.84	119.53
3	102.88	104.76	84.27	114.54	114.27
AVG	103.38	104.9233333	105.87	114.03	118.54
σ	2.3458545	3.088241139	19.40	2.106213031	3.866902292
COV	0.022690838	0.029433311	0.18	0.018470152	0.032621993

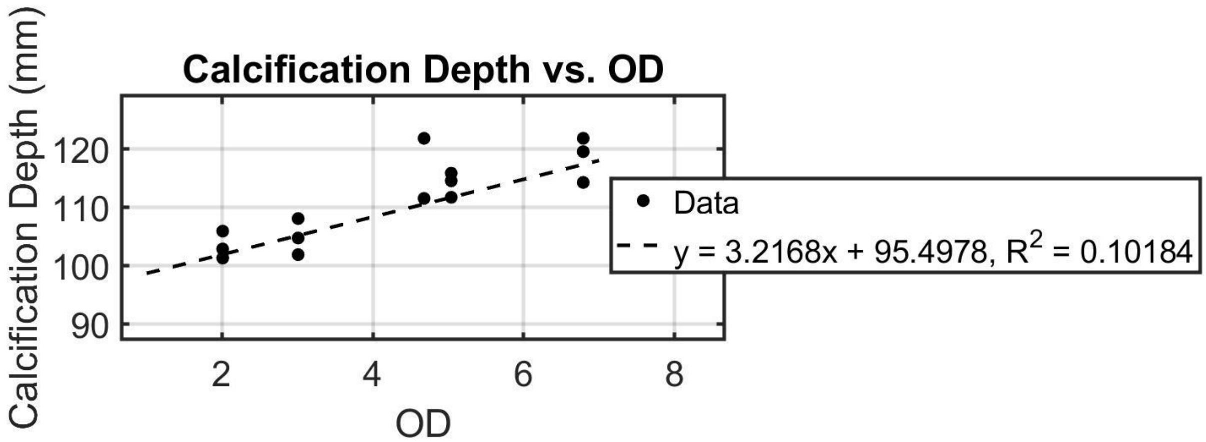

Figure 3-3. Calcification Depth vs. OD

3.1.5 OD Calcium Carbonate Content vs. PET Depth

Finally, the data was manipulated to demonstrate the calcium carbonate content versus the PET depth. Results are presented below in Figure 3-4.

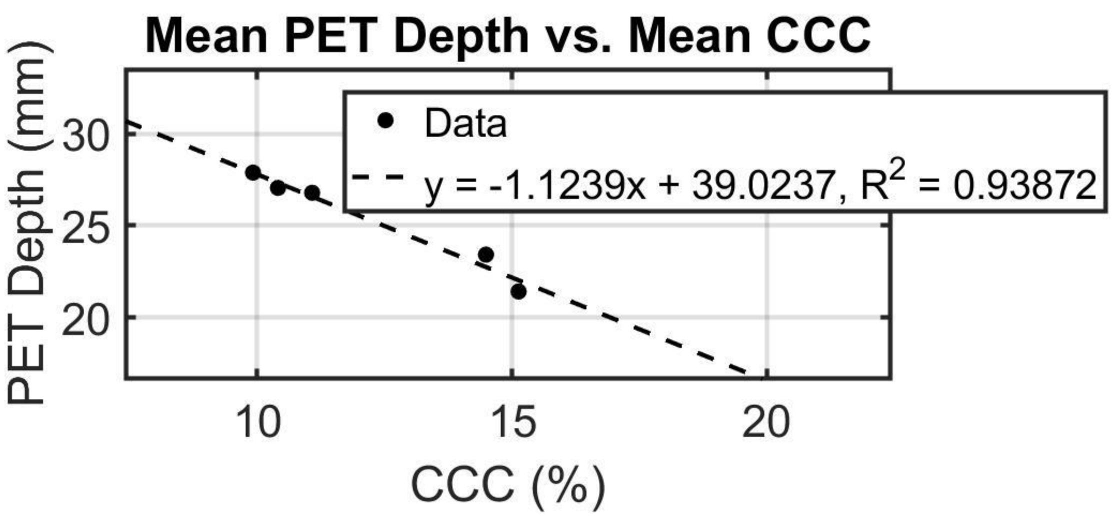

Figure 3-4. PET Depth vs. CCC (%)

3.2 Saturation Test Results

Results from the saturation study are presented below:

3.2.1 Various Saturation Level Characteristics

After staruation testing, the samples appeared similar in color, but the fully saturated samples qualitatively appeared harder and more durable as opposed to the samples that were

25% saturated. The lower saturated samples (25%, 38%, etc.) qualitatively looked like beach sand at low tide, dry, packed, and slightly compacted but easily broken apart.

3.2.2 Saturation PET Depth Results

The sandboxes were treated at varying saturation levels and subjected to several PETs. Prior to testing, the pocket erodomoeter's jet velocity was verified again. Jet velocity was approximately 8.13 m/s which is still within the appropriate jet range described by Briaud et al. (2011). Five PET erosion tests were conducted on each of the sandboxes to ensure repeatability. Table 3-4, Table 3-5, and Table 3-6 illustrate the PET depth average, σ, and COV for each OD. The PET depth for each OD was plotted as a function of varying saturation percentages (S) with a best-fit regression line and is illustrated in Figure 3-5.

Table 3-4. PET Results, OD 2.01

OD: 2.01					
% SAT:	100% SAT	75% SAT	62.5% SAT	50% SAT	25% SAT
Test #	PET DEPTH (mm)	PET DEPTH (mm)	PET DEPTH (mm)	PET DEPTH (mm)	PET DEPTH (mm)
1	25.01	32.01	29.65	36.13	36.13
2	27.84	30.1	33.26	34.31	34.31
3	29.31	30.41	33.82	39.85	39.85
4	28.41	32.58	34.15	35.76	35.76
5	28.82	29.86	33.15	37.09	37.09
AVG	27.88	30.99	32.81	36.63	36.63
σ	1.69	1.22	1.81	2.06	2.06
COV	6.07	3.94	5.52	5.62	5.62

Table 3-5. PET Results, OD 3.01

OD 3.01							
% SAT:	100% SAT	90% SAT	60% SAT	50% SAT	40% SAT	38% SAT	25% SAT
Test #	PET DEPTH (mm)	PET DEPTH (mm)	PET DEPTH (mm)	PET DEPTH (mm)	PET DEPTH (mm)	PET DEPTH (mm)	PET DEPTH (mm)
1	26.79	30.33	32.32	36.58	38.72	35.9	38.19
2	28.87	29.9	33.73	34.32	35.65	36.88	36.97
3	26.11	32.32	32.33	34.33	36.22	37.09	40.86
4	26.73	29.18	33.94	33.42	34.25	37.16	36.48
5	26.74	29.31	34.38	37.67	36.64	36.92	37.53
AVG	27.05	30.21	33.34	35.26	36.3	36.79	38.01
σ	1.06	1.27	0.96	1.78	1.63	0.51	1.72
COV	3.9	4.2	2.87	5.05	4.49	1.39	4.52

Table 3-6. PET Results, OD 5.04

% SAT:	100% SAT	85.5% SAT	62.5% SAT	50% SAT	37% SAT	25% SAT
Test #	PET DEPTH (mm)	PET DEPTH (mm)	PET DEPTH (mm)	PET DEPTH (mm)	PET DEPTH (mm)	PET DEPTH (mm)
1	23.01	24.05	25.49	26.29	30.27	33.27
2	23.4	25.14	25.81	27.99	29.61	32.28
3	24.5	23.65	26.36	30.61	30.94	31.33
4	23.06	24.87	26.47	26.41	29.21	32.57
5	23.1	25.85	25.83	26.89	29.42	31.91
AVG	23.41	24.71	25.99	27.64	29.89	32.27
σ	0.63	0.88	0.41	1.79	0.71	0.73
COV	2.67	3.54	1.58	6.48	2.37	2.25

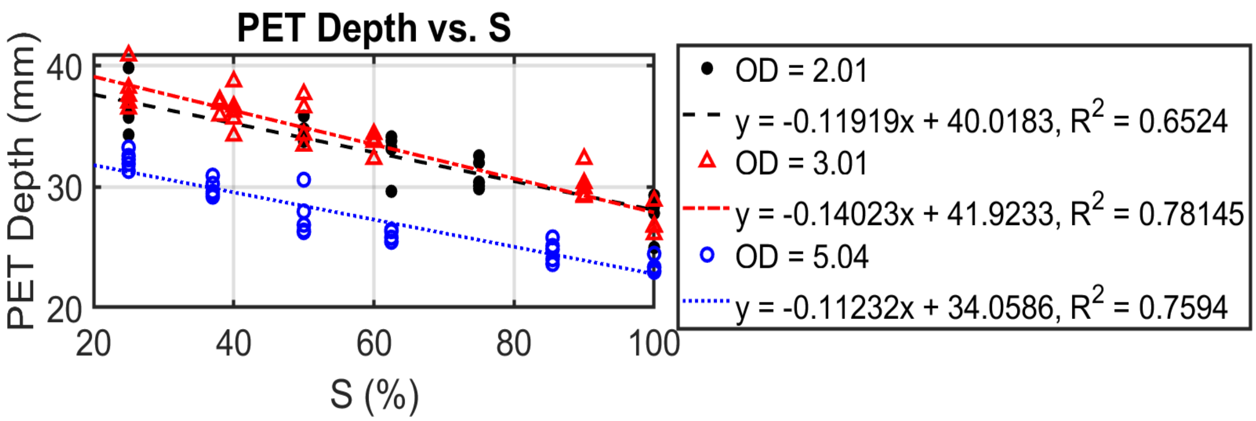

Figure 3-5. PET Depth (mm) vs. Saturation (%)

3.2.3 Saturation Calcification Results

Following the PET, the Calcium Carbonate Content (CCC) test was conducted as outlined in Chapter 2. Four CCC tests were conducted on the top surface of each of the sandboxes. The CCC results from each sandbox, the average, σ, and COV were recorded and 5.11% was deducted from the results so that only MICP-induced calcium carbonate was reported in the data, results are shown below in Table 3-7, Table 3-8, Table 3-9.

Table 3-7. Calcium Carbonate Content test results for varying saturation levels (OD: 2.01)

	100% SAT			75% SAT			62.5% SAT			50% SAT			25% SAT		
TEST #	sand sample (g)	post treated sand (g)	CCC (%)	sand sample (g)	post treated sand (g)	CCC (%)	sand sample (g)	post treated sand (g)	CCC (%)	sand sample (g)	post treated sand (g)	CCC (%)	sand sample (g)	post treated sand (g)	CCC (%)
1	5	4.23	10.29	5.01	4.26	9.86	5.02	4.27	9.83	4.99	4.3	8.718	5.02	4.35	8.24
2	5.02	4.24	10.43	5.01	4.29	9.26	5.02	4.29	9.43	5.01	4.27	9.66	5.01	4.33	8.46
3	5.01	4.29	9.26	5	4.27	9.49	4.99	4.28	9.12	5	4.3	8.89	5	4.31	8.69
4	4.99	4.27	9.32	5	4.24	10.09	4.99	4.25	9.72	5.01	4.29	9.261	5.01	4.34	8.26
AVG	5.01	4.26	9.82	5.01	4.27	9.68	5.01	4.27	9.53	5.00	4.29	9.13	5.01	4.33	8.41
σ	0.01	0.03	0.62	0.01	0.02	0.37	0.02	0.02	0.32	0.01	0.01	0.42	0.01	0.02	0.21
COV	0.00	0.01	0.06	0.00	0.00	0.04	0.00	0.00	0.03	0.00	0.00	0.05	0.00	0.00	0.03

Table 3-8. Calcium Carbonate Content test results for varying saturation levels (OD: 3.01)

	100% SAT			90% SAT			60% SAT			50% SAT		
TEST #	sand sample (g)	post treated sand (g)	CCC (%)	sand sample (g)	post treated sand (g)	CCC (%)	sand sample (g)	post treated sand (g)	CCC (%)	sand sample (g)	post treated sand (g)	CCC (%)
1	5.01	4.22	10.66	5.01	4.21	10.86	5.02	4.29	9.43	5.01	4.33	8.46
2	5.02	4.23	10.63	5.02	4.25	10.23	5.01	4.3	9.06	5	4.32	8.49
3	5	4.24	10.09	5	4.27	9.49	5.02	4.33	8.64	4.99	4.3	8.72
4	5.01	4.26	9.86	4.99	4.24	9.92	5	4.31	8.69	5.03	4.35	8.41
AVG	5.01	4.24	10.31	5.01	4.24	10.12	5.01	4.31	8.95	5.01	4.33	8.52
σ	0.01	0.02	0.40	0.01	0.02	0.58	0.01	0.02	0.37	0.02	0.02	0.14
COV	0.00	0.00	0.04	0.00	0.01	0.06	0.00	0.00	0.04	0.00	0.00	0.02

	40% SAT			38% SAT			25% SAT		
TEST #	sand sample (g)	post treated sand (g)	CCC (%)	sand sample (g)	post treated sand (g)	CCC (%)	sand sample (g)	post treated sand (g)	CCC (%)
1	5.03	4.42	7.02	5	4.34	8.09	5	4.42	6.49
2	5.03	4.36	8.21	5	4.4	6.89	4.99	4.39	6.91
3	5	4.32	8.49	5.01	4.37	7.66	4.99	4.34	7.92
4	5	4.37	7.49	5.02	4.41	7.04	5	4.39	7.09
AVG	5.02	4.37	7.80	5.01	4.38	7.42	5.00	4.39	7.10
σ	0.02	0.04	0.67	0.01	0.03	0.56	0.01	0.03	0.60
COV	0.00	0.01	0.09	0.00	0.01	0.08	0.00	0.01	0.08

Table 3-9. Calcium Carbonate Content test results for varying saturation levels (OD: 5.04

	100% SAT			85.5% SAT			62.5% SAT		
TEST #	sand sample (g)	post treated sand (g)	CCC (%)	sand sample (g)	post treated sand (g)	CCC (%)	sand sample (g)	post treated sand (g)	CCC (%)
1	4.98	3.98	14.97	5.02	4.19	11.42	4.99	4.29	8.92
2	5.01	4.29	9.26	5.03	4.2	11.39	5.01	4.29	9.26
3	5	4.24	10.09	5.03	4.29	9.60	5	4.3	8.89
4	5.03	4.29	9.60	5	4.28	9.29	5.01	4.28	9.46
AVG	5.01	4.20	10.98	5.02	4.24	10.43	5.00	4.29	9.13
σ	0.02	0.15	2.68	0.01	0.05	1.14	0.01	0.01	0.28
COV	0.00	0.04	0.24	0.00	0.01	0.11	0.00	0.00	0.03

	50% SAT			37% SAT			25% SAT		
TEST #	sand sample (g)	post treated sand (g)	CCC (%)	sand sample (g)	post treated sand (g)	CCC (%)	sand sample (g)	post treated sand (g)	CCC (%)
1	4.99	4.34	7.92	5.01	4.25	10.06	5	4.35	7.89
2	5.03	4.28	9.80	5.04	4.34	8.78	5.01	4.37	7.66
3	5.01	4.29	9.26	4.99	4.36	7.52	5	4.32	8.49
4	4.99	4.3	8.72	5.02	4.39	7.44	4.99	4.34	7.92
AVG	5.01	4.30	8.92	5.02	4.34	8.45	5.00	4.35	7.99
σ	0.02	0.03	0.80	0.02	0.06	1.24	0.01	0.02	0.35
COV	0.00	0.01	0.09	0.00	0.01	0.15	0.00	0.00	0.04

Figure 3-6 illustrates the CCC as a function of the various saturation levels applied to each OD.

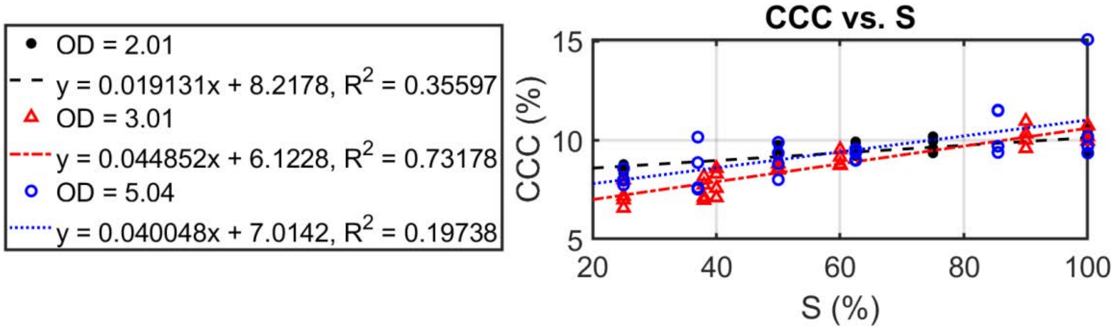

Figure 3-6. CCC (%) vs. Saturation (%)

3.2.4 Saturation Treatment Depth Test

Results from strong calcification testing are shown below in Table 3-10, Table 3-11, and Table 3-12. Each table represents a different OD.

Table 3-10. MICP application depths for varying Saturation Levels (OD: 2.01)

% Sat:	100% SAT	75% SAT	62.5% SAT	50% SAT	25% SAT
TEST #	MICP APPLICATION DEPTH (mm)	MICP APPLICATION DEPTH (mm)	MICP APPLICATION DEPTH (mm)	MICP APPLICATION DEPTH (mm)	MICP APPLICATION DEPTH (mm)
1	101.33	90.29	83.70	76.34	35.04
2	105.94	96.97	81.12	76.74	36.01
3	102.88	94.36	82.89	67.63	34.60
AVG	103.38	93.87	82.57	73.57	35.21666667
σ	2.3458545	3.366486794	1.319431696	5.148077311	0.721410655
COV	0.022690838	0.035862014	0.015979553	0.069975225	0.020484922

Table 3-11. MICP application depths for varying Saturation Levels (OD: 3.01)

% Sat:	100% SAT	90% SAT	75% SAT	60% SAT	50% SAT	40% SAT	38% SAT	25% SAT
TEST #	MICP APP. DEPTH (mm)	MICP APP. DEPTH (mm)	MICP APP. DEPTH (mm)	MICP APP. DEPTH (mm)	MICP APP. DEPTH (mm)	MICP APP. DEPTH (mm)	MICP APP. DEPTH (mm)	MICP APP. DEPTH (mm)
1	108.09	104.31	96.87	86.84	79.77	43.35	40.58	38.1
2	101.92	101.72	94.72	85.01	78.13	40.35	42.29	34.87
3	104.76	102.54	96.04	84.98	78.72	44.48	41.96	43.25
AVG	104.92	102.86	95.87	85.61	78.87	42.72	41.61	38.74
σ	3.088	1.323	1.084	1.065	0.831	2.134	0.907	4.226
COV	0.029	0.012	0.011	0.012	0.010	0.049	0.021	0.109

Table 3-12. MICP application depths for varying Saturation Levels (OD: 5.04)

% SAT:	100% SAT	85.5% SAT	62% SAT	50% SAT	37% SAT	25% SAT
TEST #	MICP APP. DEPTH (mm)	MICP APP. DEPTH (mm)	MICP APP. DEPTH (mm)	MICP APP. DEPTH (mm)	MICP APP. DEPTH (mm)	MICP APP. DEPTH (mm)
1	111.72	103.08	82.83	80.91	70.91	51.21
2	115.84	100.74	87.74	79.98	68.26	50.78
3	114.54	112.38	84.72	80.16	70.05	53.58
AVG	114.03	105.40	85.10	80.35	69.74	51.86
σ	2.11	6.16	2.48	0.49	1.35	1.51
COV	0.02	0.06	0.03	0.01	0.02	0.03

Figure 3-7 illustrates each OD's average strong calcification depth as a function of saturation levels (S) with best-fit regression lines:

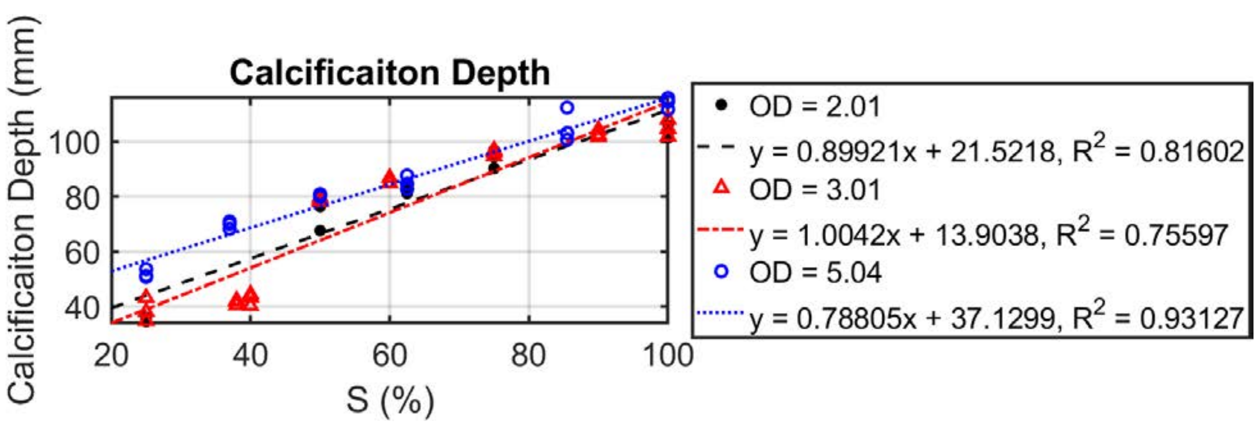

Figure 3-7. Calcification Depth vs. Saturation (%)

3.2.5 Saturation Calcification vs. PET Depth

Finally, the three OD (2.01, 3.01, and 5.04) CCC results were combined and compared to the average PET depth at varying saturation levels. The results and best-fit regression equations are presented in Figure 3-8.

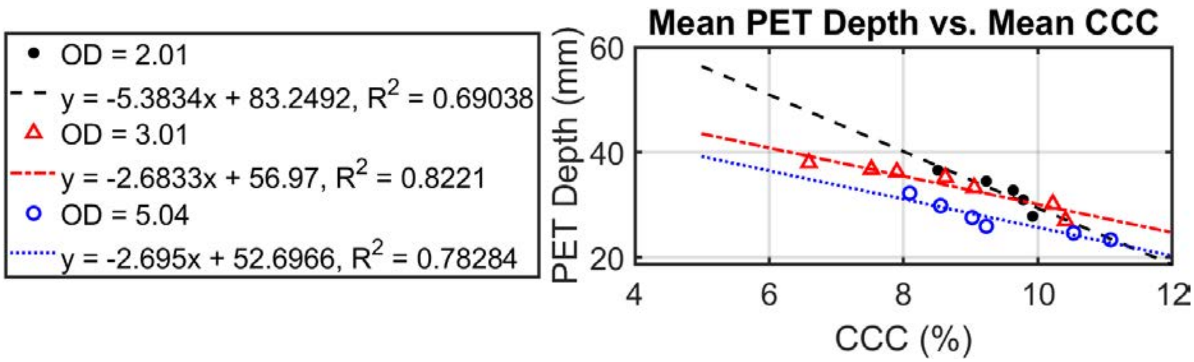

Figure 3-8. PET depth (mm) vs. CCC (%)

3.3 Food Ratio Test Results Test Results

Results from the food ratio study are presented below:

3.3.1 Food Ratio Characteristics

After testing, visual inspection indicated that the boxes that were treated with a 0.25:1.75 ratio (12.5% bacteria and 87.5% feedstock) appeared to resemble moistened sand with very little calcification whereas the 1:1 ratio boxes quantitatively looked as though calcification had occurred.

3.3.2 Food Ratio PET Depth Test Results

The first test conducted on the food ratio study was the PET. Like the previous tests, the pocket erodometer's jet velocity was verified. This time the jet velocity was approximately 7.93 m/s which is still within the appropriate jet range (Briaud et al. 2011). Five PET erosion tests were conducted on each of the sandboxes to ensure repeatability. Table 3-13 illustrates the PET depth average, σ, and COV for each of the four food ratio tests conducted.

Table 3-13. PET results from food ratio study. (OD: 4.68)

OD: 4.68				
RATIOS:	1:1	0.75 : 1.25	0.5 : 1.5	0.25 : 1.75
Test #	PET DEPTH (mm)	PET DEPTH (mm)	PET DEPTH (mm)	PET DEPTH (mm)
1	26.38	26.69	40.52	43.34
2	25.46	26.41	41.1	40.97
3	26.1	25.5	35.71	39.71
4	27.85	26.21	38.05	38.98
5	28.12	24.68	43.76	39.74
AVG	26.782	25.898	39.828	40.548
σ	1.1517	0.81066	3.069066633	1.716615857
COV	4.3001	3.130204	7.70580153	4.233540142

Figure 3-9 illustrates the PET depth versus the food ratio content (plotted as as volume of voids occupied by *S. pasteurii)* with a best-fit regression equation.

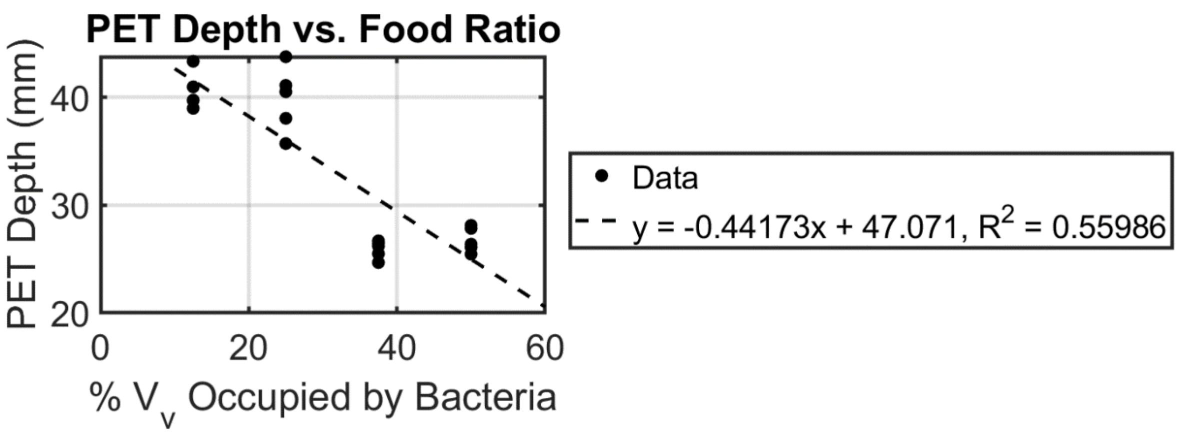

Figure 3-9. PET depth (mm) vs. Food Ratio

3.3.3 Food Ratio Calcification Results

Following the PET, the Calcium Carbonate Content (CCC) test was performed. Four CCC tests were conducted on the top surface of each of the sandboxes. The CCC results of each sandbox, their average, σ, and COV were recorded and 5.11% was deducted from the results so that only MICP-induced calcium carbonate was reported in the data, results are shown below in Table 3-14.

Table 3-14. Calcium Carbonate Content test results for food study ratio (OD: 4.68)

OD: 4.68												
RATIO:	1:1			0.75 : 1.25			0.5 : 1.5			0.25 : 1.75		
TEST #	sand sample (g)	post treated sand (g)	CCC (%)	sand sample (g)	post treated sand (g)	CCC (%)	sand sample (g)	post treated sand (g)	CCC (%)	sand sample (g)	post treated sand (g)	CCC (%)
1	5.01	3.95	16.05	5	3.97	15.49	4.99	4.41	6.51	5	4.5	4.89
2	5.01	4.37	7.66	5.03	4.01	15.17	5	4.44	6.09	5.01	4.5	5.07
3	5.04	4.34	8.78	4.99	3.99	14.93	5.01	4.41	6.87	5.01	4.35	8.06
4	5.01	4.14	12.26	4.99	4	14.73	5	4.38	7.29	5.02	4.4	7.24
AVG	5.02	4.20	11.19	5.00	3.99	15.08	5.00	4.41	6.69	5.01	4.44	6.32
σ	0.02	0.20	3.78	0.02	0.02	0.33	0.01	0.02	0.51	0.01	0.08	1.58
COV	0.00	0.05	0.34	0.00	0.00	0.02	0.00	0.01	0.08	0.00	0.02	0.25

A plot illustrating the CCC as a function of the food ratio is shown below in Figure 3-10:

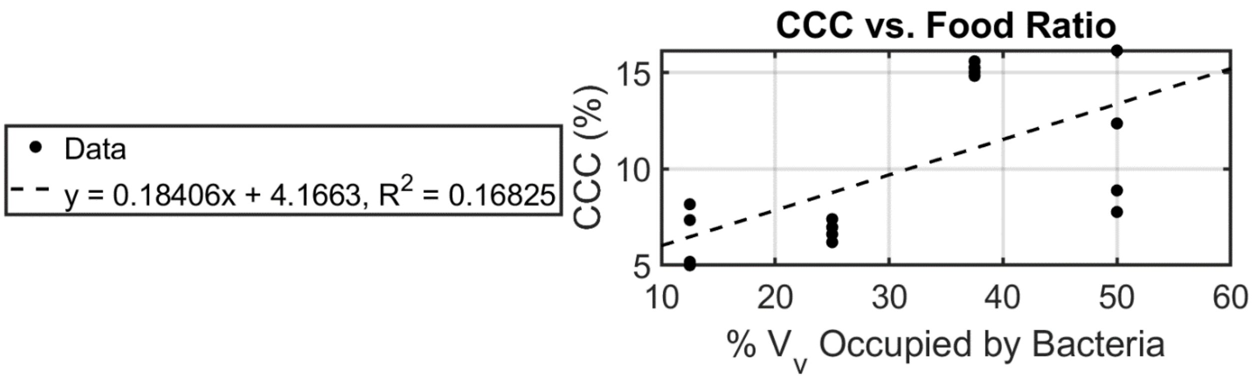

Figure 3-10. CCC (%) vs. Food Ratio

3.3.4 Food Ratio Treatment Depth Test

After the PET and CCC tests, the sandboxes were again disassembled so that the side profile could be observed and measured. The depth of strong calcification was measured with a caliper in the center and along either side of the sandboxes. The results were averaged and are outlined in Table 3-15 below:

Table 3-15. Strong Calcification depths for varying Food Ratios

Food Ratio Test -- OD 4.68				
RATIO:	1:1	0.75 : 1.25	0.5 : 1.5	0.25 : 1.75
TEST #	MICP APPLICATION DEPTH (mm)	MICP APPLICATION DEPTH (mm)	MICP APPLICATION DEPTH (mm)	MICP APPLICATION DEPTH (mm)
1	121.81	99.51	88.71	56.13
2	111.53	98.73	82.42	53.54
3	84.27	100.56	91.38	57.13
AVG	105.87	99.60	87.50	55.60
σ	19.40	0.92	4.60	1.85
COV	0.18	0.01	0.05	0.03

Figure 3-11 illustrates the calcification depths as a function of the V_v occupied by the *S. pasteurii* bacteria with a best-fit regression line below:

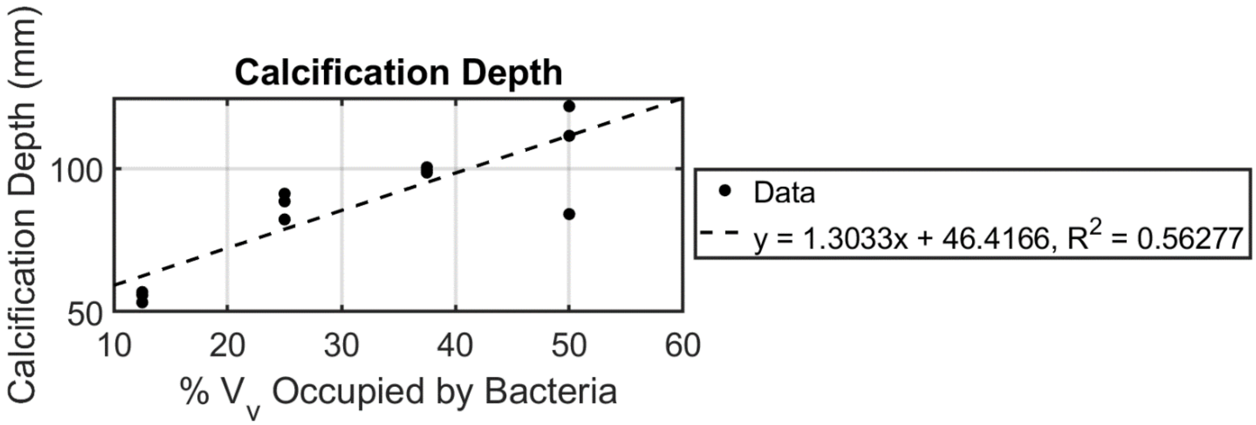

Figure 3-11. Calcification depth vs. Food Ratio

3.3.5 Food Ratio Calcification vs. PET Depth

The results from the four food ratio parameters were combined to compare the calcium carbonate content to the average erosion depths. The results are presented in Figure 3-12.

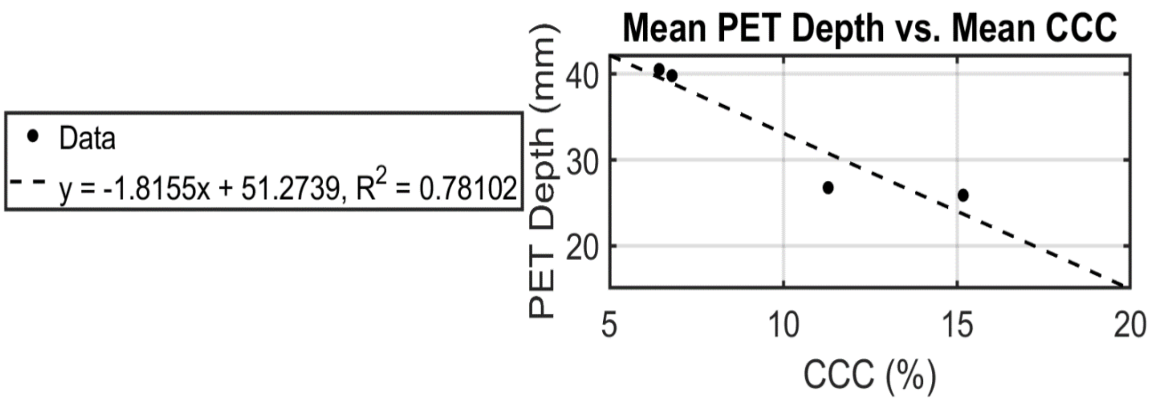

Figure 3-12. PET depths (mm) vs. CCC (%)

3.4 Multiple Treatment Test Results

Results from the multiple treatment test were as follows:

3.4.1 Multiple Treatment Test Characteristics

After testing, the samples appeared similar in color, but the samples with multiple treatments appeared to exhibit a harder and more-calcified surface layer than the box with only one treatment. The boxes with multiple treatments had a much more potent odor than those specimens with one or two treatments.

3.4.2 Multiple Treatment PET Depth Results

PET jet velocity was approximately 8.41 m/s which is within the appropriate jet range (Briaud et al. 2011). Table 3-16 illustrates the PET depth average, standard deviation, and coefficient of variation for each of the five sandboxes.

Table 3-16. PET Results, Multiple Treatments

# TREATMENTS:	ONE TREATMENT	TWO TREATMENTS	THREE TREATMENTS	FOUR TREATMENTS	FIVE TREATMENTS
Test #	PET DEPTH (mm)	PET DEPTH (mm)	PET DEPTH (mm)	PET DEPTH (mm)	PET DEPTH (mm)
1	27.38	25.56	22.32	18.51	10.29
2	27.46	27.41	21.17	14.98	11.95
3	28.1	25.24	20.81	16.48	12.93
4	27.85	25.32	18.84	18.61	9.22
5	28.12	24.94	20.99	17.92	9.37
AVG	27.782	25.694	20.826	17.3	10.752
σ	0.348	0.985	1.257	1.551	1.632
COV	1.254	3.832	6.036	8.964	15.175

Figure 3-13 (below) illustrates the PET depths as a function of number of treatments, N, with a best-fit regression line. Results are consistent with the original hypothesis that more treatments will decrease the erodibility.

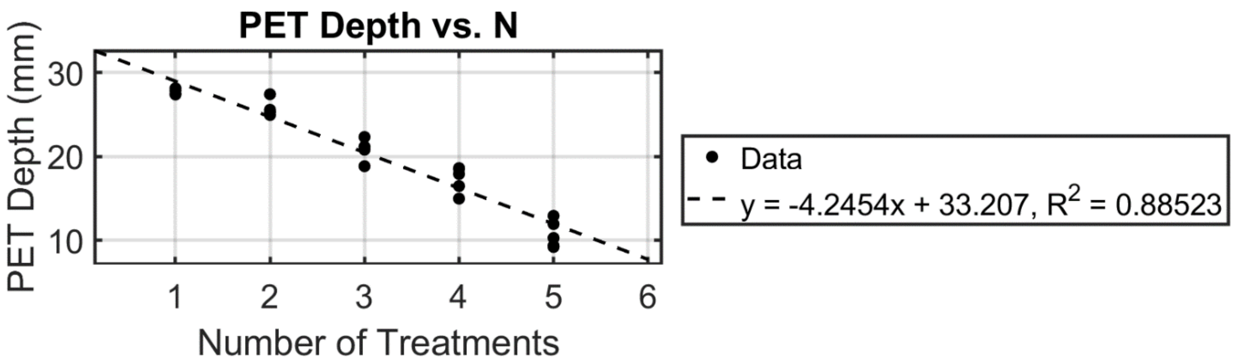

Figure 3-13. PET depth vs. Number of treatments

3.4.3 Multiple Calcification Results

Results from CCC testing are presented below in Table 3-17 and Figure 3-14:

Table 3-17. CCC Results, Multiple Treatments

TEST #	ONE TREATMENT			TWO TREATMENTS			THREE TREATMENTS			FOUR TREATMENTS			FIVE TREATMENTS		
	sand sample (g)	post treated sand (g)	CCC (%)	sand sample (g)	post treated sand (g)	CCC (%)	sand sample (g)	post treated sand (g)	CCC (%)	sand sample (g)	post treated sand (g)	CCC (%)	sand sample (g)	post treated sand (g)	CCC (%)
1	5.06	4.08	14.26	5.05	4.03	15.09	4.99	3.99	14.93	5.02	4.01	15.01	5.01	3.9	17.05
2	4.99	4	14.73	5	4	14.89	5.01	4.01	14.85	5.04	4.01	15.33	5.03	3.99	15.57
3	5.01	4.07	13.65	4.99	4.01	14.53	4.99	3.99	14.93	5.02	3.9	17.20	5.02	3.92	16.80
4	4.99	3.99	14.93	5.01	4	15.05	5	3.95	15.89	5.04	3.99	15.72	5.01	3.95	16.05
AVG	5.01	4.04	14.39	5.01	4.01	14.89	5.00	3.99	15.15	5.03	3.98	15.82	5.02	3.94	16.37
σ	0.03	0.05	0.57	0.03	0.01	0.25	0.01	0.03	0.49	0.01	0.05	0.97	0.01	0.04	0.68
COV	0.01	0.01	0.04	0.01	0.00	0.02	0.00	0.01	0.03	0.00	0.01	0.06	0.00	0.01	0.04

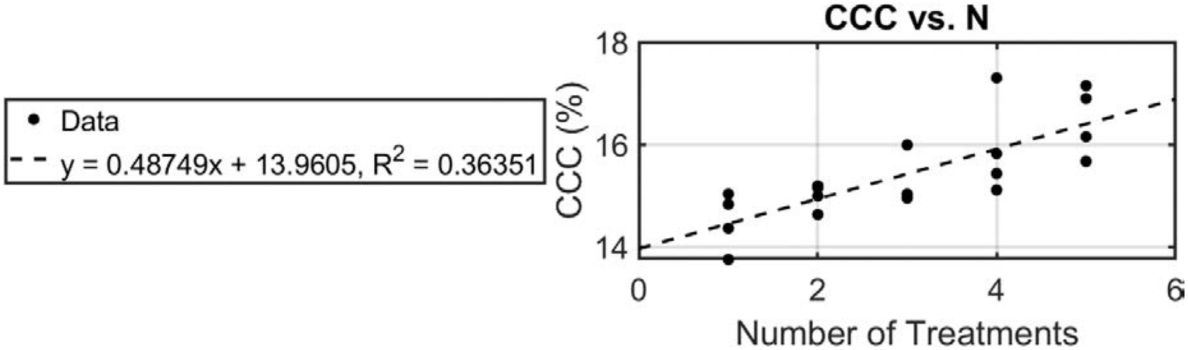

Figure 3-14. CCC (%) vs. Number of Treatments (N)

3.4.4 Multiple Treatment Depth Test

. Figure 3-15 is a photograph from the multiple treatment depth test. The results were averaged and are outlined in Table 3-18 below:

Figure 3-15. Multiple treatment sandboxes

Table 3-18. MICP application depths for multiple treatment test

# TREATMENTS:	ONE TREATMENT	TWO TREATMENTS	THREE TREATMENTS	FOUR TREATMENTS	FIVE TREATMENTS
TEST #	MICP APPLICATION DEPTH (mm)	MICP APPLICATION DEPTH (mm)	MICP APPLICATION DEPTH (mm)	MICP APPLICATION DEPTH (mm)	MICP APPLICATION DEPTH (mm)
1	100.57	114.73	116.88	127.67	131.11
2	101.60	110.17	117.25	128.96	130.31
3	101.14	113.93	117.58	130.32	130.47
AVG	101.10	112.94	117.24	128.98	130.63
σ	0.52	2.43	0.35	1.33	0.42
COV	0.01	0.02	0.00	0.01	0.00

The calcification depth averages as a function of number of treatments and a best-fit regression line are illustrated in Figure 3-16 below:

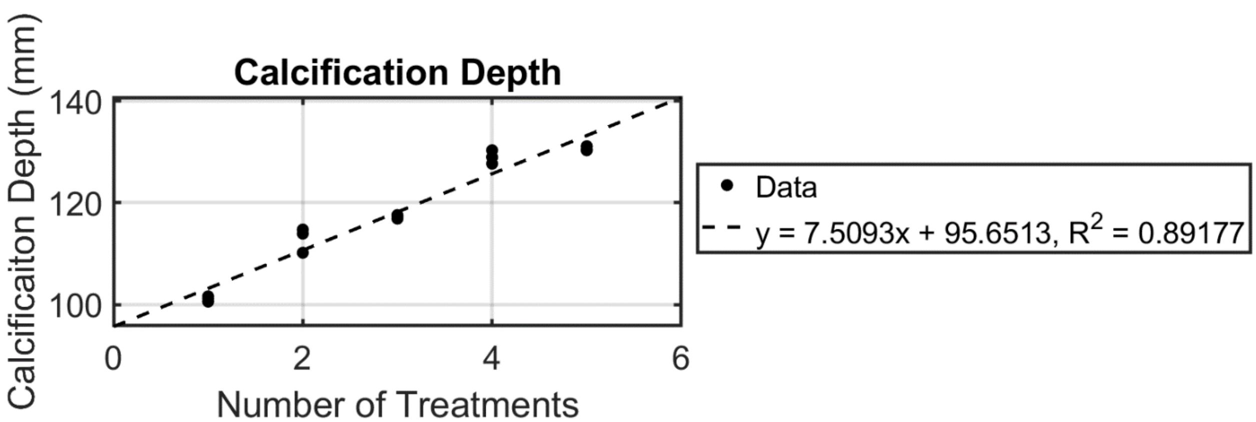

Figure 3-16. Calcification depth (mm) vs. number of treatments

3.1.5 Multiple Treatment Calcification vs. PET Depth

Finally, the data was manipulated to illustrate the calcium carbonate content versus the average PET depth. The results and best-fit regression equation are presented in Figure 3-17 below:

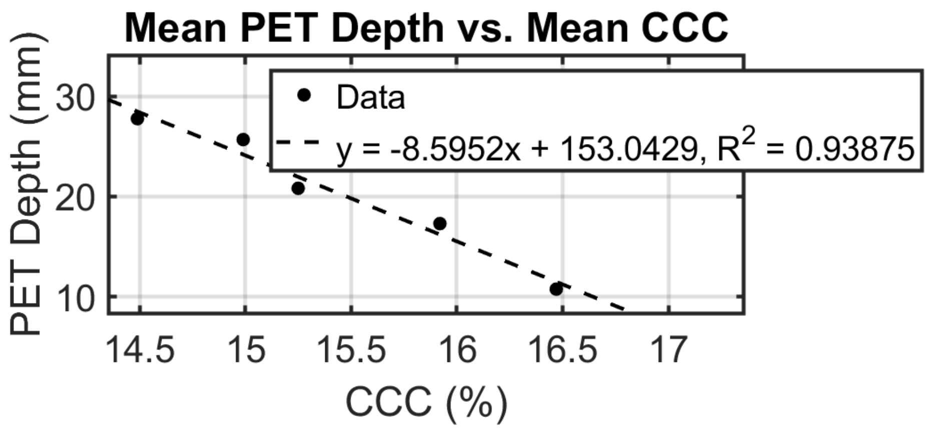

Figure 3-17. Mean PET Depth vs. Mean CCC

CHAPTER 4
DISCUSSION

Results appeared to confirm investigators' initial hypotheses. Specifically, higher concentrations of *Sporosarcina pasteurii* combined with higher saturation levels and/or multiple treatments produced erosion improvement for MICP-treated beach sand specimens that was greater than erosion improvement achieved using lower-concentration constituents. This chapter analyzes the results from each study and the variables' effects on erodibility and calcification. Following the analysis is a discussion regarding upscaling for field application.

4.1 Data Analysis

Results from the saturation study indicated that as saturation levels (S) increased, the PET depth decreased. However, these improvements were small after one surface-spray treatment. Untreated beach sand is known to be "Category I: Very High Erodibility." Even at the "optimized treatment level" (i.e., most saturated) one MICP treatment was only able to improve erosion to "Category II: High Erodibility" (Briaud et al. 2011). Likewise, the results from the study illustrate that as saturation levels increase, the CCC percentages also increase. Lastly, the study illustrates that the calcification depth is also a function of saturation levels; samples treated with greater saturation percentages showed greater calcification depths.

Similarly, results from the OD testing illustrated that as the OD increased, the PET depth decreased; however, the results remain in the "High Erodibility" category (Briaud et al. 2011). Comparable to the saturation study, as the OD increased the CCC percentages also increased. Finally, and again comparable to the saturation study, as the OD increased, the calcification depth of the sandboxes also increased.

The food ratio study results indicated that the PET depth decreased as bacteria (relative to food) was added to the specimens. But these samples were all still classified as "Category II:

High Erodibility" (Briaud et al. 2011). Additionally, the CCC percentages increased as the sample boxes approach a 1:1 stoichiometrically balanced ratio. Finally, the results showed that the samples occupied by more urea/$CaCl_2$ and less bacteria had lower calcification depths than those that were stoichiometrically balanced.

The multiple treatment test results showed that multiple treatments may significantly decrease erodibility. After five treatments, specimens could be classified as "Category III: Medium Erodibility" (Briaud et al. 2011). As expected, more treatments led to more calcification and deeper calcification depth.

Figure 4-1 is a compilation of each study where PET depth is shown as a function of CCC. As illustrated, there appears to be an indirect relationship between these two variables.

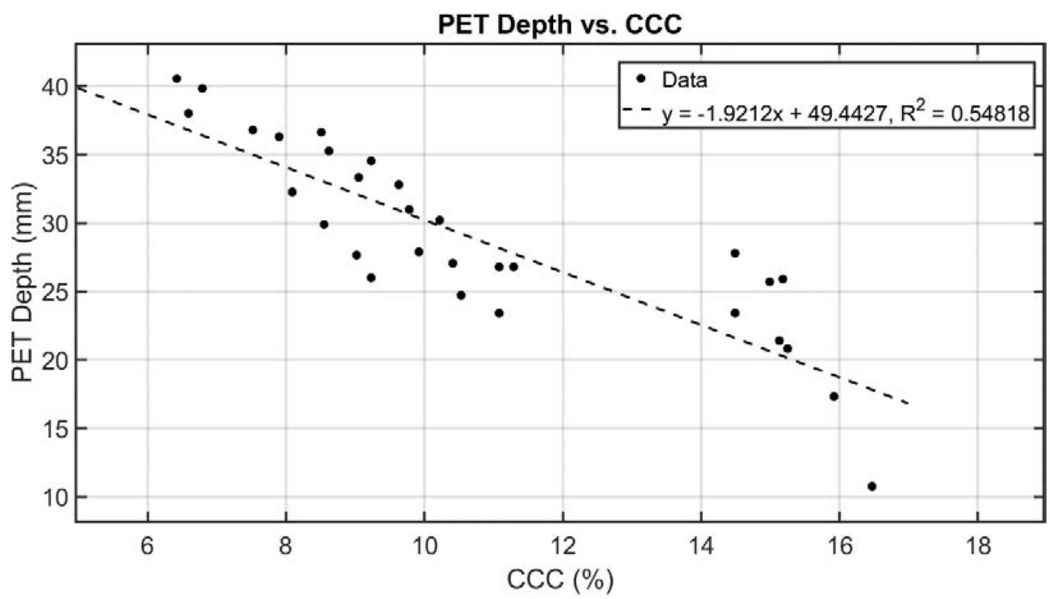

Figure 4-1. Compilation of all tests PET depth (mm) vs. CCC (%)

4.2 Research Comparision

Nafisi and Montoya (2018) treated specimen with ODs ranging between 0.8 to 1.2 using a two-phase injection method. Cementation treatments were repeated, and the direction of injection was alternated to improve calcium carbonate distribution. Like the research presented in this thesis, Nafisi & Montoya (2018) used an acid washing technique with 1 M HCL solution to determine the calcium carbonate content. Despite the extra effort in alternating the injection direction throughout the application process, results from their research concluded calcium carbonate percentages ranged from 2.6% to 7.2% depending on the type of sand (i.e. Ottawa 20-30, Ottawa 50-70, and Nevada sand). Nafisi and Montoya (2018) showed that more calcium carbonate was needed to bind particles and reach a specific level of cementation, but they, were unable to increase the carbonate percentages sufficiently to decrease the erodibility.

Montoya et al. (2018) results showed that MICP treatment could reduce erodibility, but to decrease erodibility significantly, multiple treatments were needed. Specimens were treated with urea (0.33 M), ammonium chloride (0.374 M) and relatively small amounts of calcium chloride (0.05 M). Initial bacterial ODs ranged between 1.0 and 1.2. Based on the results, the average mass of calcium carbonate (m_c) were 1.0% for lightly cemented, 2.6% for moderately cemented, and 4.8% for heavily cemented specimens respectively. Additionally, Montoya et al. (2018) results were compared results from previous Erosion Function Apparatus (EFA) tests. Lightly cemented specimen (i.e., m_c 1.0%) were categorized as "Category I: Very High Erodibility;" moderately cemented specimen (i.e., m_c 2.6%) were categorized as "Category II: High Erodibility;" and heavily cemented specimen (i.e., m_c 4.8%) were categorized as "Category III: Medium Erodibility." Montoya et al. (2018) results indicated that 1~ 2% may be the threshold level of cementation for minimizing the erodibility of the sands using those parameters and treatment application techniques. As many as 30 treatments were required to achieve "heavy cementation" (Montoya et al. 2018).

Ghasemi et al. (2019) quantified erodibility as a function of relative concentrations of urea and calcium chloride. The study used *Sporosarcina pasteurii* bacteria with ODs ranging between 0.8 to 1.2 and the urea used varied between 2 and 3 M. A surface percolation method was used to treat the unsaturated specimens. The soils used were Ottawa 20-30 sand and a natural North Carolinian soil. The calcium carbonate content was determined by gravimetric acid washing. Results showed that greater erodibility improvements were achieved for higher relative urea concentrations. However, the calcium carbonate content only reached a maximum of 11.92% with some specimen only reaching 2.65% during UCS compressive tests (Ghasemi et al. 2019).

Unlike these previous MICP erosion studies, this study used *Sporosarcina pasteurii* bacteria with much higher ODs ranging from a minimum of 2.01 to maximum OD of 6.79. This high OD bacteria solution was given significant urea and bacteria. This technique is different from techniques that other MICP researchers are using and appears to be effective. During this study, CCC percentages were at least 6% after only one treatment (after accounting for the 5% calcium carbonate already present in the beach sand) and after five treatments, CCC was as high as 16%. In other words, the techniques, presented here appeared to be more effective after one treatment than previous techniques after several treatments – at least in terms of surface calcification. Finally, multiple treatments appeared to be the most significant method to improve results further and increase CCC.

PET results were less encouraging than results from the CCC tests. When this study began, investigators' goal had been to reduce erodibility for beach sand from its known starting point – Category I: Very High Erodibility – to something resembling relatively effective erosion resistance – Category III: Medium Erodibility or better, using only one treatment. Previous studies in erosion rate testing (Bloomquist et al. 2012; Crowley et al. 2012; Crowley et al. 2012; Crowley et al. 2012; Crowley et al. 2014) have shown that achieving erosion resistance with a bed stress of ~100 Pa usually means relatively erosion-resistant material that will reasonably withstand scour. Unfortunately, none of the MICP-treated specimens were able to achieve "medium erodibility" after only one treatment. Instead, even after optimization/maximization of the MICP constituents studied here, five treatments were required to achieve "medium erodibility." At the same time, as indicated above, these results appear to be an improvement when compared with previous work, and they appear to indicate that required CCC associated with achieving significant erosion resistance may be higher than previously thought. Results presented here appear to indicate that medium erodibility requires at least 14% CCC whereas Montoya et al. (2018) indicated that aforementioned 1 ~ 2% threshold.

4.3 Implications for Upscaling for Field Application

Results from Briaud et al. (2011) show that a bed stress of 100 Pa corresponds to "medium erodibility" and an expected erosion rate of 100 mm/hr. Likewise, results from this study show that specimens with the highest OD, maximized bacteria as a function of pore volume, optimized ratio between urea/calcium chloride and bacteria, and treated five times were only able to achieve medium erodibility and the effective treatment depth was, on-average approximately 130 mm. Combing the two sets of data appears to indicate that during high stress ~100 Pa stress events such as waves associated with a hurricane or a nor'easter, one might expect to lose any benefit associated with MICP treatment relatively quickly – in a little over an hour. In other words, while localized erosion benefits associated with MICP treatment may be achievable, they may be short-lived in the context of large-scale field events.

However, this does not mean that MICP is a completely ineffective erosion treatment technique. Unlike the sandboxes used during this study, a beach dune effectively has an infinite pore volume associated with it. In this context, the "more is better" results associated with this study could be extrapolated. In other words, to maximize erosion resistance one should spray a dune with as much bacteria as possible; at as high an OD as possible; and give the bacteria as much food as possible. Future work should be aimed at better-approximating this infinity condition and at examining other heartier bacteria that can lyse urea and are easier than *S. pasteurii* to mass-produce.

CHAPTER 5
CONCLUSIONS

To summarize, investigators hypothesized that erodibility associated with MICP-treated natural beach sand specimens may be governed by (1) OD; (2) S; and (3) ratio between bacteria and urea/calcium chloride when a surface spray technique was used to treat the sand. Several series of experiments were conducted to determine the effects of these variables on MICP effectiveness in terms of erodibility, resultant CCC, and calcification depth. Results showed the following:

- Higher OD led to higher CCC, less erosion, and deeper calcification.
- More bacteria relative to V_v led to higher CCC, less erosion, and deeper calcification.
- More bacteria relative to urea/calcium chloride led to higher CCC, less erosion, and deeper calcification.

In addition, correlations were developed between erodibility and CCC; and strong calcification depth and CCC. Overall, results showed indirect relationships between CCC and PET depth; and direct relationships between CCC and calcification depth. Overall, holistically, results lead to the conclusion that varying OD and increasing bacteria quantity – both in terms of the relative amounts of bacteria compared to urea/calcium chloride and in terms of its relative quantity as a function of void ratio – may have significant effects on CCC and subsequently erodibility.

LIST OF REFERENCES

Alizadeh, A., 1974, "Amount and Type of Clay and Pore Fluid Influences on The Critical Shear Stress and Swelling of Cohesive Soils," Ph.D. dissertation, University of California, Davis.

Al-Madhhachi, A. S. T., Hanson, G. J., Fox, G. A., Tyagi, A. K., & Bulut, R. (2013). Measuring soil erodibility using a laboratory "mini" JET. *Transactions of the ASABE*, *56*(3), 901-910.

Anderson, M. Science Encyclopedia. *Beach Nourishment,* 2009. Accessed November 3, 2019 from : http://science.jrank.org/pages/780/Beach-Nourishment.html.

Arneson, L. A. (2013). *Evaluating scour at bridges* (No. FHWA-HIF-12-003). United States. Federal Highway Administration.

ASTM (2014). "Standard Test Method for Rapid Determination of Carbonate Content of Soils," ASTM International West Conshohocken, PA.

ASTM (2014). "Standard Test Methods for Specific Gravity of Soil Solids by Water Pycnometer", ASTM International West Conshohocken, PA.

ASTM (2014). " Standard Test Method for Sieve Analysis of Fine and Coarse Aggregates", ASTM International West Conshohocken, PA.

Bloomquist, D., Sheppard, D. M., Schofield, S., and Crowley, R. W. (2012). "The Rotating Erosion Testing Apparatus (RETA): A Laboratory Device for Measuring Erosion Rates versus Shear Stresses of Rock and Cohesive Materials." *Geotechnical Testing Journal*, 35(4), 641-648.

Briaud, J., MBernhardt, M., and Leclair, M. (2011). "The Pocket Erodometer Test: Development and Preliminary Results " *Geotechnical Testing Journal*, 35(2), 342-352.

Briaud, J.-L., Ting, F., Checn, H. C., Cao, Y., Han, S.-W., and Kwak, K. (2001). "Erosion Function Apparatus for Scour Rate Predictions." *Journal of Geotechinal and Geoenvironmental Engineering*, 127(2), 105-113.

Briaud, J. L., 2008, “Case Histories in Soil and Rock Erosion: Woodrow Wilson Bridge, Brazos River Meander, Normandy Cliffs, and New Orleans Levees,” J. Geotech. Geoenviron.Eng., Vol. 134, No. 10, pp. 1424–1447.

Brown, S. A., & Clyde, E. S. (1989). *Design of riprap revetment* (No. FHWA-IP-89-016). United States. Federal Highway Administration.

Bruun, P., 1954. Coast erosion and the development of beach profiles. Technical Memorandum No. 44, Beach Erosion Board, U.S. Army Corps of Engineers.

Bush, D. M., Longo, N. J., Neal, W. J., Lindeman, K. C., Pilkey, D. F., Esteves, L. S., ... & Pilkey Jr, O. H. (2004). *Living with Florida's Atlantic beaches: coastal hazards from Amelia Island to Key West*. Duke University Press.

Chapius, R., and Gatien, T., 1986, “An Improved Rotating Cylinder Technique for Quantitative Measurements of the Scour Resistance of Clays,” Can. J. Geotech. Eng., Vol. 23, 83–87.

Cheng, L., Cord-Ruwisch, R., & Shahin, M. A. (2013). Cementation of sand soil by microbially induced calcite precipitation at various degrees of saturation. *Canadian Geotechnical Journal*, *50*(1), 81-90.

Choi, S.-G., Park, S.-S., Wu, S., and Chu, J. (2017). "Methods for Calcium Carbonate Content Measurement of Biocemented Soils." 29(11), 06017015.

Crowley, R., Bloomquist, D., and Robeck, C. "Description of Erosion Rate Testing Devices and Correlations between Rock Erosion Rate and Cohesion." *Proc., 6th International Conference on Scour and Erosion*.

Crowley, R., Bloomquist, D., Shah, F. D., and Holst, C. M. (2012). "The Sediment Erosion Rate Flume (SERF): A New Testing Device for Measuring Soil Erosion Rate and Shear Stress." *Geotechincal Testing Journal*, 35(4).

Crowley, R., Davies, M., Ellis, T. N., Hudyma, N., Ammons, P., and Matemu, C. "Microbial Induced Calcite Precipitation of Dune Sand using a Surface Spray Technique." *Proc., Geo-Congress 2019*.

Crowley, R. W., Bloomquist, D., Hayne, J. R., Holst, C. M., and Shah, F. D. (2012). "Estimation and Measurement of Bed Material Shear Stresses in Erosion Rate Testing Devices." *Journal of Hydraulic Engineering-Asce*, 138(11), 990-994.

Crowley, R. W., Bloomquist, D. G., and Sheppard, D. M. (2014). "Investigation of Erosion Rates of Field Samples Using FDOT's Enhanced Sediment Erosion Rate Flume (SERF)." Florida Department of Transportation, Tallahassee, FL.

Dean, R. G. (2003). *Beach nourishment: theory and practice* (Vol. 18). World Scientific Publishing Company.

De Jong, J. T., Martinez, B. C., Mortensen, B. M., Nelson, D. C., Waller, J. T., Weil, M. H., Ginn, T. R., Weathers, T. S., Barkouki, T. H., Fujita, Y., Redden, G., Hunt, C., Major, D., and Tanyu, B. (2009). "Upscaling of Bio-Mediated Soil Improvement." *17th International Conference on Soil Metchanics and Geotechnial Engineering*.

DeJong, J. T., Fritzges, M. B., and Nusslein, K. (2006). "Microbially Induced Cementation to Control Sand Response to Undrained Shear." *Journal of Geotechinal and Geoenvironmental Engineering*, 132(11), 1381-1392.

DeJong, J. T., Mortensen, B. M., Martinez, B. C., and Nelson, D. C. (2010). "Bio-Mediated Soil Improvement." *Ecological Engineering*, 36(2), 197-210.

DeJong, J. T., Soga, K., Kavazanjian, E., Burns, S., van Paassen, L. A., Al Qabany, A., Aydilek, A., Bang, S. S., Burbank, M., Caslake, L. F., Chen, C. Y., Cheng, X., Chu, J., Ciurli, S., Esnault-Filet, A., Fauriel, S., Hamdan, N., Hata, T., Inagaki, Y., Jefferis, S., Kuo, M., Laloui, L., Larrahondo, J., Manning, D. A. C., Martinez, B. C., Montoya, B. M., Nelson, D. C., Palomino, A., Renforth, P., Santamarina, J. C., Seagren, E. A., Tanyu, B., Tsesarsky, M., and Weaver, T. (2013). "Biogeochemical Processes and Geotechnial Applications: Progress, Opportunities, and Challenges." *Geotechnique*, 63(4), 287-301.

Einstein, H. A., and Krone, R. B. (1962). "Experiments to Determien Modes of Cohesive Sedimetn Transport in Salt Water." *Journal of Geophysical Research*, 67(4), 1451-1461.

Fauriel, S., & Laloui, L. (2013). Biogeochemical processes and geotechnical applications: progress, opportunities and challenges. *Geotechnique-London-*, *63*(ARTICLE), 287-301

Federal Emergency Management Agency (FEMA). Engineering with nature: alternative techniques to riprap bank stabilization. Retrieved September18, 2019 from: https://www.fema.gov/pdf/about/regions/regionx/Engineering_With_Nature_Web.pdf

Fuller, J. (2017). Strength Property Variability in Microbial Induced Calcite Precipitation Soils.

Ghasemi, P., Zamani, A., and Montoya, B. M. "The Effect of Chemical Concentration of the Strength and Erodibility of MICP Treated Sands." *Proc., Geo-Congress 2019*, 241-249.

Green, K. B. Florida Department of Environmental Protection. *State of Florida Strategic Beach Management Plan,* June, 2019. http://www.dep.state.fl.us/beaches/publications/pdf/int-sbmp.pdf. Accessed October 5, 2019.

Hanson, G. J. (1990). "Surface Erodibility of Earthen Channels at High Stresses Part II - Devleop and In Situ Testing Device." *Transactions of the ASAE*, 33(1), 132-137.

Hanson, G. J., and Cook, K. R. (1997). "Development of Excess Shear Stress Parameters for Circular Jet Testing." *ASAE Annual International Meeting*Minneapolis, MN.

Hanson, G. J. S., A. (2001). "Erodibility of Cohesive Streambeds in teh Loess Area of the Midwestern USA." *Hydrological Processes*, 15, 23-38.

Lee, S. C., & Mehta, A. J. (1994). *Cohesive sediment erosion*. FLORIDA UNIV GAINESVILLE DEPT OF COASTAL AND OCEANOGRAPHIC ENGINEERING.

Maleki, M., Ebrahimi, S., Asadzadeh, F., and Emami Tabrizi, M. (2016). "Performance of microbial-induced carbonate precipitation on wind erosion control of sandy soil." *International Journal of Environmental Science and Technology*, 13(3), 937-944.

Martinez, B. C., and DeJong, J. T. "Bio-Mediated Soil Improvement: Load Transfer Mechanisms at the Micro- and Macro-Scales." *Proc., US-Cina Workshop on Ground Improvement Technologies, ASCE GSP*, 10.

Massey, W. (2017). *Assessing the impact of riprap bank stabilization on fish habitat: A study of Lowland and Appalachian streams in Southern Québec* (Doctoral dissertation, Concordia University).

Mehta, A. J. "Review Notes on Cohesive Sediment Erosion." *Proc., Geology*.

Mobley, H. L. T., Island, M. D., and Hausinger, R. P. (1995). "Molecular Biology of Microbial Ureases." *Microbiological Reviews*, 59(3), 31.

Montoya, B. M., Do, J., and Gabr, M. "Erodibility of Microbial Induced Carbonate Preciptiation-Stabilized Sand under Submerged Impinging Jet." *Proc., IFCEE 2018 GSP 296*.

Montoya, B. M., & DeJong, J. T. (2015). Stress-strain behavior of sands cemented by microbially induced calcite precipitation. *Journal of Geotechnical and Geoenvironmental Engineering*, *141*(6), 04015019.

Moore, W.L. and Masch, F.D., “Experiments on the scour resistance of cohesive sediments.” *Journal of Geophysical Research*, Vol. 67, No. 4, 1962, pp. 1437-1449.

Mortensen, B. M., Haber, M. J., DeJong, J. T., Caslake, L. F., and Nelson, D. C. (2011). "Effects of environmental factors on microbial induced calcium carbonate precipitation." *Journal of applied microbiology*, 111(2), 338-349.

Mujah, D., Shahin, M. A., & Cheng, L. (2017). State-of-the-art review of biocementation by microbially induced calcite precipitation (MICP) for soil stabilization. *Geomicrobiology Journal*, *34*(6), 524-537.

Nafisi, A., & Montoya, B. M. (2018). A new framework for identifying cementation level of MICP-treated sands. In *IFCEE 2018* (pp. 37-47).

Ng, W.-S., Lee, M.-L., and Hii, S.-L. (2012). "An Overview of the Factors Affecting Microbial-Induced Calcite Precipitation and its Potential Application in Soil Improvement." *International Journal of Civil, Environmental, Structural, Construction and Architectural Engineering*, 6(2), 188-194.

Ranasinghe, R., I. Turner and G. Symonds, 2006. Shoreline Response to Submerged Structures: A review. Coastal Engineering, 53: 65-79.

Rektorik, R. J., and Smerdon, E. T., June 1964, “Critical Shear Stress in Cohesive Soils from a Rotating Shear Stress Apparatus,” Paper No. 64-216, American Society of Agricultural Engineers Annual Meeting, Fort Collins, CO., June 21–24.

Salifu, E., MacLachlan, E., Iyer, K. R., Knapp, C. W., and Tarantino, A. (2016). "Applicaiton of Microbially Induced Calcite Precipitation in Erosion Mitigation and Stabilisation of Sandy Soil for Foreshore Slopes: A Preliminary Investigation." *Engineering Geology*, 201, 96-105.

Sargunam, A., Riley, P., Arulanandan, K., and Krone, R. B., March 1973, “Effect of Physicochemical Factors on the Erosion of Cohesive Soils,” J. Hydraul. Div., Vol. 99, HY3, pp. 555–558.

Shanahan, C., and Montoya, B. M. "Erosion Reduction of Coastal Sands using Microbial Induced Calcite Precipitation " *Proc., Geo-Chicago 2016*.

Sharma, A., & Ramkrishnan, R. (2016). Study on effect of Microbial Induced Calcite Precipitates on strength of fine-grained soils. *Perspectives in Science*, *8*, 198-202.

Shehata, W. M., and M. H. Al-Rehaili. (2005). “A Review of Sand Dune Stabilization.” *ResearchGate*

Shields, A. F. (1936). "Applciation of Similarly Principles and Turbulence Research to Bed-Load Movement." CalTech, Pasadena, CA.

Soon, N. W., Lee, L. M., Khun, T. C., & Ling, H. S. (2013). Improvements in engineering properties of soils through microbial-induced calcite precipitation. *KSCE Journal of Civil Engineering*, *17*(4), 718-728.

U.S. Department of Transportation Federal Highway Administration. (1989). Design of riprap revetment. Accessed: October 17, 2014 from: http://www.fhwa.dot.gov/engineering/hydraulics/pubs/hec/hec11sI.pdf

Van Paassen, Leon A., Claudia M. Daza, Marc Staal, Dimitri Y. Sorokin, Willem van der Zon, and Mark CM van Loosdrecht. "Potential soil reinforcement by biological denitrification." *Ecological Engineering* 36, no. 2 (2010): 168-175.

Weil, M. H., DeJong, J. T., Martinez, B. C., and Mortensen, B. M. (2012). "Seismic and Resistivity Measurements for Real-Time Monitoring of Microbially Induced Calcite Precipitation in Sand." *Geotechincal Testing Journal*, 35(2).

Whiffin, V. S., van Paassen, L. A., & Harkes, M. P. (2007). Microbial carbonate precipitation as a soil improvement technique. *Geomicrobiology Journal*, *24*(5), 417-423.

Zhao, Q., Li, L., Li, C., Li, M., Amini, F., & Zhang, H. (2014). Factors affecting improvement of engineering properties of MICP-treated soil catalyzed by bacteria and urease. *Journal of Materials in Civil Engineering*, *26*(12), 04014094.

BIOGRAPHICAL SKETCH

Abigail Chek was born and raised in Jackson, New Jersey and a 2014 graduate of the United States Naval Academy. She earned a Bachelor of Science in Ocean Engineering and was commissioned as an ensign on May 23, 2014. Since graduation in 2014, Abigail's operational and shore assignments include: Naval Mobile Construction Battalion ONE, where she served as Detachment Guam Company Commander, Detail Pensacola Officer in Charge, and Convoy Security Element Commander; and Public Works Department Naval Station Norfolk, where she served as a waterfront construction manager.

Abigail is qualified as a Professional Engineer (PE) in the State of Michigan. She was selected into the NAVFAC Ocean Facilities Program in 2017 and since August 2018, Abigail has been a graduate student in the Master of Civil/Coastal Engineering program at the University of North Florida in Jacksonville, Florida. Upon completion of graduate school, Abigail will have follow on orders to the Naval Diving and Salvage Training Center in Panama City, Fl where she will become a qualified Navy Diving Officer.